https://ntrs.nasa.gov/search.jsp?R=19830021440 2020-03-21T02:14:22+00:00Z

nasa TM-81698

NASA Technical Memorandum 81698

NASA-TM-81698 19830021440

Experimental Investigations of Elastohydrodynamic Lubrication

Bernard J. Hamrock
Lewis Research Center
Cleveland, Ohio

and

Duncan Dowson
The University of Leeds
Leeds, England

LIBRARY COPY

JUL 14 1983

LANGLEY RESEARCH CENTER
LIBRARY, NASA
HAMPTON, VIRGINIA

NASA
National Aeronautics and Space Administration
Lewis Research Center

1983

ENTER:
10 1 1 RN/NASA-TM-81698
DISPLAY 10/2/1
83N29711** ISSUE 18 PAGE 2947 CATEGORY 37 RPT#: NASA-TM-81698
E-209 NAS 1.15:81698 83/05/00 102 PAGES UNCLASSIFIED DOCUMENT
UTTL: Experimental investigations of elastohydrodynamic lubrication
AUTH: A/HAMROCK, B. J.; B/DOWSON, D. PAA: B/(Leeds Univ., England)
CORP: National Aeronautics and Space Administration. Lewis Research Center, Cleveland, Ohio. AVAIL.NTIS SAP: HC A06/MF A01
Repr. from Ball Bearing Lubrication, Sep. 1981
MAJS: /*ELASTOHYDRODYNAMICS/*LUBRICATION/*PARAMETER IDENTIFICATION
MINS: / CAPACITANCE/ INTERFEROMETRY/ THIN FILMS
ABA: Author
ABS: Various experimental studies of elastohydrodynamic lubrication have been reviewed. The various types of machines used in these investigations, such as the disc, two and four ball, crossed-cylinders, and crossed-axes rolling disc machine, are described. The measurement of the most important parameters, such as film shape, film thickness, pressure, temperature, and traction, is considered. Determination of the film thickness is generally the most important of these effects since it dictates the extent to which the asperities on opposing surfaces can come into contact and thus has a direct bearing on wear and fatigue failure of the contacting surfaces. Several different techniques for measuring film thickness have been described, including electrical resistance, capacitance, X-ray, optical interferometry, laser beam diffraction, strain gage, and spring
ENTER:
DISPLAY 10/2/1
dynamometer methods. An attempt has been made to describe the basic concepts and limitations of each of these techniques. These various methods have been used by individual researchers, but there is no universally acceptable technique for measuring elastohydrodynamic film thickness. Capacitance methods have provided most of the reliable data for nominal line or rectangular conjunctions, but optical interferometry has proved to be the most effective procedure for elliptical contacts. Optical interferometry has the great advantage that it reveals not only the film thickness, but also details of the film shape over the complete area of the conjunction.

EXPERIMENTAL INVESTIGATIONS OF ELASTOHYDRODYNAMIC LUBRICATION*

Some of the most important variables involved in experimental research on elastohydrodynamic lubrication are film thickness, traction, pressure, and temperature. The distribution of these variables in the conjunction has been studied by a number of investigators. These studies and the apparatus used in measuring these effects are considered in this chapter. Of these considerations the determination of the film thickness in the lubricated conjunction is a most significant aspect of elastohydrodynamic lubrication. Film thickness dictates the extent to which the asperities on opposing surfaces can come into contact and thus has a direct bearing on the wear and fatigue failure of contacting surfaces.

Nearly all experimental work on elastohydrodynamic lubrication has been carried out since 1950. However, long before that time operating experience with gears and other highly loaded lubricated contacts had suggested that the solids might be separated by a fluid film under some conditions. Much of the evidence was indirect and inconclusive, but the persistence of machining marks and the lack of serious surface damage provided the strongest case in support of some form of fluid-film lubri-

---

*Published as Chapter 10 in Ball Bearing Lubrication by Bernard J. Hamrock and Duncan Dowson, John Wiley & Sons, Inc., Sept. 1981.

N83-29711#

cation. In addition, the measured efficiency of gears suggested that the friction force generated in the gear tooth contact was more representative of fluid-film conditions than of boundary friction or metallic contact.

10.1 Apparatus

Many different forms of apparatus have been used in the study of elastohydrodynamic lubrication, and some of these have been designed primarily for measuring film thickness. The apparatus used has been developed to accommodate the different geometrical forms of elastohydrodynamically lubricated contacts, namely, rectangular, elliptical, or circular. It is also vital to consider the kinematics of the bounding solids since the film thickness generated depends on half the vector sum of the velocities of the two surfaces ($(u_a + u_b)/2$, the entraining velocity) and the bulk of the energy dissipation depends on the vector difference of these two velocities ($u_a - u_b$, the sliding velocity). The "sliding-entraining ratio" defined as $2(u_a - u_b)/(u_a + u_b)$ is an important dimensionless velocity ratio, particularly when traction is considered. Each form of apparatus is therefore assessed in terms of the flexibility in the geometrical form and the kinematic conditions of the conjunction that can be tested. The results obtained from these various forms of experimental apparatus have been used extensively in developing design pro-

cedures for gears, ball and roller bearings, cams, and tappets and in analyzing both the performance and failure of such lubricated machine elements.

10.1.1 Disc Machines

The lubrication of nominal line or rectangular contacts has generally been investigated by using various modifications of the disc machine first used by Merritt (1935) to measure the coefficient of friction in simulated gear-tooth contact conditions. In Merritt's machine two discs were pressed together with a known force and rotated at known speeds. The torque due to friction was then measured by a dynamometer. The two discs were selected to represent any particular contact geometry, and the two shafts carrying the test discs were chain driven to provide various combinations of sliding and rolling velocities. The work reported by Merritt (1935) provided valuable data on friction in simulated gear tooth contacts. Various modifications of the disc machine have made it a standard piece of equipment for examining highly loaded rectangular contacts.

A disadvantage of the conventional two-disc machine is that it is not particularly convenient for measuring rolling friction near the rolling point. The bearing friction can be very much larger than the frictional traction between the discs under these circumstances. In the four-disc machine shown in Figure

10.1 and devised by Crook (1963) these small tractions can be measured because the central disc is unrestrained except for an air-thrust block that provides axial location. However, the conventional four-disc machine in which the free central disc is braked can be used only for sliding speeds up to the value at which the maximum traction occurs. The more conventional and versatile two-disc machine has been used over a much wider range of sliding-entraining ratios.

10.1.2 Four-Ball Machine

The four-ball machine has been one of the most widely used forms of apparatus in lubrication studies. The test pieces are four balls that are held in the form of a pyramid by a conforming race. The upper ball is held by a collet and driven by an electric motor through pulleys and a timing belt. The platform holding the lower race is raised when load is applied so that the upper ball fits centrally into the triangle formed by the lower three balls. In some forms of the machine the three lower balls are held stationary (sliding four-ball machine), but in others the lower balls are allowed to roll around the race (rolling four-ball machine) such that the upper ball is in effect the inner race of a special form of ball bearing.

As an apparatus for the detailed study of elastohydrodynamic lubrication the four-ball machine suffers from three major

defects. First, the kinematic conditions are inflexible and complex. The sliding-entraining ratio $2(u_a - u_b) / (u_a + u_b)$ is not always representative of motions within realistic lubricated machine elements, particularly in the sliding four-ball machine, and the conjunction is subjected to a spin component of velocity. Second, it has a low thermal capacity, which makes the surface temperature very difficult to control. Third, because the contact areas remain stationary on the lower balls in the sliding four-ball machine, these surfaces could wear under more severe conditions so as to achieve a greater degree of conformity.

10.1.3 Two-Ball Machine

Any combination of rolling and sliding can be considered in a general form of the two-ball machine, shown in Figure 10.2. The two steel balls are normally mounted at the respective ends of two vertical spindles. Both spindles can rotate at different speeds and in the same or opposite directions as required. Conditions of combined sliding, rolling, and spin in the contact can thus be produced, making this a more flexible apparatus for studying lubrication of circular contacts than the conventional four-ball machine. One of the first investigators to use the two-ball machine was Lane (1951), who sought to simulate the failure of gears due to scuffing.

The main frame of the two-ball machine consists essentially of two parts coupled by a horizontal hinge so that the upper part can be tilted back to provide ready access to the lower part of the machine. Each part of the machine carries a spindle, hollow at one end, into which the test pieces are secured by means of special chucks. When the two halves are closed together, the two balls are brought into contact and the load between them can be varied by means of weights.

10.1.4 Crossed-Cylinders Machine

One disadvantage of any apparatus using spheres, or balls, is the difficulty of manufacturing the test specimens to be exactly spherical. In some cases, however, precision balls produced for ball bearings can be used, provided that they can be mounted satisfactorily. This particular problem can be overcome neatly by using a crossed-cylinders configuration. Figure 10.3 shows the essential parts of the crossed-cylinders machine used by Archard and Kirk (1961). The lower cylinder (or specimen) rotates and also traverses slowly to and fro so that the point of contact traces out a helical path on both specimens. Because the two rotations and the traverse are not synchronous, all parts of the specimens have an opportunity to be presented to the conjunction between the rotating components.

The lower specimen is mounted on a carriage that is moved to and fro by a hydraulic ram whose speed is continuously varied. At each rotational speed the traversal speed is adjusted so that there is no overlapping of the helical track traced out by the contact area. The length of the traverse is controlled by electrical limit switches, and an experiment can be performed on any selected portion of the specimens. The rotation of the lower specimen is effected through a telescopic shaft and flexible couplings. The lower specimen assembly is insulated from the body of the machine so that the electrical capacity and electrical resistance between the specimens can be measured. Electrical connections to the specimens themselves and to thermocouples embedded in them are made by mercury contacts. The upper specimen is mounted on an arm that is pivoted at one end in a gimbal mounting.

10.1.5 Crossed-Axes Rolling Disc Machine

A disadvantage of the crossed-cylinders machine is that the kinematic conditions are somewhat inflexible. If the rotational speed is large compared with the traversal speed, the sliding-entraining ratio is always close to 2. In the crossed-axes rolling disc apparatus used by Smith (1959) a range of conditions is possible. In this machine, shown in Figure 10.4, the lower specimen is rotated and the upper specimen rolls freely on

it, driven by the viscous stresses transmitted through the elastohydrodynamic film. A range of sliding-entraining ratios is possible, the variation being achieved by changing the angle between the axes of the upper and lower specimens.

10.2 Film Thickness Measurements

To achieve a satisfactory procedure for measuring film thickness in elastohydrodynamically lubricated contacts, it is necessary to adopt a system that can be calibrated over the range of very small separations between the solids. Furthermore the calibration must take account of the fact that realistic elastohydrodynamic conjunctions are filled, fully or partially, by a lubricant whose properties may vary considerably under the severe physical conditions encountered between the solids. Such calibrations can be difficult to perform in practice because of the small film thicknesses (fractions of a micrometer, or several microinches) encountered and the difficulty in establishing these known film thicknesses and shapes accurately by mechanical methods. The techniques of film thickness measurement that have been adopted can be classified as electrical, X-ray, optical, and mechanical.

10.2.1 Electrical Techniques

Electrical Resistance Measurements

The electrical resistance measurement technique is especially useful for detecting lubricant films, but attempts have also been made to use the principle for quantitative measurements of film thickness under full and partial elastohydrodynamic conditions. It involves measuring the electrical resistance of the lubricant film and then attempting to relate this property to film thickness. The resistance drops immediately to near zero values as metal-to-metal contact is made at the asperities, but it increases in a complex manner as separation of the solids increases, and this makes it exceedingly difficult to relate resistance measurements to film thickness in a satisfactory manner.

Lane and Hughes (1952) appear to have been among the first to study oil film formation in gears by electrical resistance methods. The potential difference across insulated gears on a gear testing machine was recorded on a cathode ray oscilloscope while the gears were in motion. Although the results were necessarily qualitative because of uncertainty about the electrical properties of lubricants under contact conditions, they clearly demonstrated the existence of effective lubricating films.

Cameron (1954) noted that the electrical characteristics of an oil film depend on the current. At currents less than about 0.5 A the oil film resistance was found to depend on the applied voltage, with the oil behaving almost like an ohmic resistance. At higher currents the voltage drop across the film (i.e., the discharge voltage) was effectively constant. The possibility of relating resistance measurements to oil film thickness was discussed in detail by Lewicki (1955).

Furey (1961) also used this technique to detect the contact of asperities through an elastohydrodynamic film. In his approach two resistors formed a potentiometer across the applied voltage. The resistances were given as a ratio, and this prevented large voltages from being applied between the surfaces in contact. These resistances could be varied over a wide range while their ratio was kept constant. A relationship between the area of contact and both the speed and lubricant characteristics was obtained. It is of course necessary for the two surfaces in rolling contact to be electrically insulated, so that the only conductivity between them arises from the oil film.

The electrical resistance technique has been used to estimate the overall amount of metallic contact between rolling surfaces. It is therefore particularly useful in studying the role of surface topography in the formation and behavior of elastohydrodynamic films. For very smooth surfaces the measured electrical resistance will be almost infinite if an effective elas-

tohydrodynamic film is generated. If additives such as sodium petroleum sulphonate are added to the lubricating oil to reduce its resistivity, the disadvantages of the electrical resistance technique still persist because of the possible dependence of resistivity on pressure and temperature. Strictly speaking this method does not determine film thickness but simply indicates film breakdown in the contact. Thus it cannot be relied on for the quantitative measurement of film thickness. It is of course particularly sensitive to the presence of dirt particles in the lubricant. Nevertheless it is a measurement method that has found some application in research on the establishment of elastohydrodynamic films in rolling contact.

Capacitance Measurements

In the capacitance measurement technique the capacitance of the lubricating film between rolling contacts is measured, and the film thickness is interpreted from these measurements. The capacitance readings can be related to the permittivity of free space, the dielectric constant of the lubricant, and the surface shape and area such that an estimate can be made of the film thickness. This technique was pioneered by Crook (1958) and used most effectively by Dyson, et al. (1965-66) to measure film thickness in elastohydrodynamic contacts.

Capacitance measurement requires not only insulation of the rolling surfaces, but also extremely well-finished surfaces. This technique provides an integrated film thickness rather than a local one, although good estimates can be made of central and even minimum film thicknesses if the shape of the film is known with reasonable accuracy. Furthermore because the dielectric constant of the lubricant and its variation with pressure and temperature must be determined, preliminary calibration is needed.

The capacitance technique for measuring film thickness provided the basis for the substantial expansion of experimental studies of elastohydrodynamic lubrication in the 1960's. In this period a most satisfactory agreement between theory and experiment for line or rectangular contacts was first achieved. It is no exaggeration to say that capacitance techniques have provided the basis for most successful film thickness measurements in line contacts.

10.2.2 X-Ray Technique

A radically different approach to the measurement of film thickness was adopted by Sibley, et al. (1960) when they developed their X-ray method and their precision disc machine. Figure 10.5 shows the arrangement of the apparatus. Molybdenum X-radiation was diffracted from a lithium fluoride crystal to

obtain a collimated monochromatic beam. The size and shape of the beam were controlled by adjustable tantalum slits. This beam was then directed along the tangent plane between two lubricated rolling discs, and the emergent beam was detected with a Geiger counter. The measurement of the film thickness depends on the fact that X-rays are transmitted through the lubricant with little adsorption but are strongly adsorbed by the steel discs. The X-ray count rate measured with the Geiger counter corresponds to a given film thickness as a function of the lubricant. Figure 10.6 shows the initial calibration graph for the X-ray technique presented by Bell and Kannel (1970) for a given lubricant. The graph was obtained by mechanically setting known gaps between unloaded rolling contacts and then measuring the X-ray count rates. As this figure shows, different lubricating oils have different X-ray adsorption coefficients. The measured X-ray count rate and the initial calibration graph shown in Figure 10.6 enabled the elastohydrodynamic film thickness to be determined.

There are two problems in using this technique. The first is to ensure that the X-ray beam is sufficiently parallel and well aligned either with the plane of the common tangent to the undeformed discs or with the plane of the parallel lubricant film. Consider, for example, the following situation: A Hertzian region 0.75 mm wide is separated by a parallel film 0.25 μm thick. In this situation the X-ray beam could be com-

pletely cut off by adjusting the lower disc parallel to the beam direction by 12.5 μm. Considerable experimental expertise is needed in using this technique.

The second problem with the X-ray technique is that the initial calibration has to be carried out on unloaded discs separated by distances that are mechanically determined. Since the lubricant properties and the lengths of the effective elastohydrodynamic regions may be different under actual operating conditions, the ability to measure film thicknesses of the order of 0.5 μm by this technique can be questioned.

10.2.3 Optical Techniques

Interferometry

Optical interferometry, together with the capacitance method mentioned earlier, is the most widely used procedure for determining film thickness in experimental studies of elastohydrodynamic lubrication. Indeed interferometry has been particularly valuable in revealing the form and thickness of elastohydrodynamic films in nominal point or elliptical conjunctions. Capacitance techniques have provided the vast majority of the reliable measurements of film thickness in nominal line or rectangular conjunctions.

The apparatus used in association with the interferometry technique described by Foord, et al. (1969-70) is shown in Figure 10.7. A specially coated glass plate was mounted on an air bearing and driven by a highly finished ball mounted in a polytetrafluoroethylene (PTFE) cup. The ball was loaded against the lower surface of the disc by an air cylinder and rotated by a variable-speed electric motor. Oil was drip fed onto the ball and drawn into the contact, where an elastohydrodynamic film was generated.

The optical system used a microscope, typically with a X5 objective and a X10 eyepiece for 50 times magnification in all, and a specially designed collimator described by Foord, et al. (1969-70). As the oil films of interest were thin and relatively low magnifications were adequate, the critical points in achieving good fringe quality were the intensities of the interfering beams and the provision of a vibration-free machine to give stationary fringe patterns.

The first significant publication on the use of optical interferometry for measuring elastohydrodynamic film thickness was by Cameron and Gohar (1966). They loaded a lubricated rotating steel ball against a stationary plate of high-refractive-index glass and obtained interference patterns that revealed the now classical horseshoe-shaped constriction in elastohydrodynamic film thickness generated in a circular contact. Their use of a sliding contact and special glass imposed a severe restric-

tion on load, speed, and fringe quality. These limitations were later reduced by using sapphire and diamond as a transparent member, as reported by Gohar and Cameron (1966). A great improvement in fringe quality was obtained by Foord, et al. (1968) who, instead of relying on differences in refractive index, used a 20-percent-reflectivity layer of chromium. This allowed the transparent material to be selected for its mechanical properties and enabled the experimental conditions to be extended to pure rolling and high speeds.

A major disadvantage of optical interferometry is that it requires one of the two bodies to be a flat transparent surface and so, at best, it is only a simulation of actual bearing situations. It is desirable to have adequate simulation of both the conjunction geometry and the properties of the materials.

The refractive index of the transparent disc and the oil must be determined. Furthermore the surface finish of the metallic ball should be extremely fine (<0.025 μm (1 μin.) Ra). Otherwise an inferior interference pattern is produced. This poses problems in studies of low-film-thickness regimes, where asperity geometry is significant. These various effects tend to cause differences between the experimental situation and the actual conditions observed in bearings. Nevertheless, optical interferometry is of immense value in research on fundamental aspects of elastohydrodynamic lubrication, and the technique has

been used effectively to extend our understanding of the phenomenon.

A new procedure based on measurements of intensity changes in optical interferometry, which was developed initially for dealing with rough surfaces (Swingler, 1980), appears to offer considerable scope for the enhancement of film thickness measurements in elastohydrodynamic conjunctions.

Laser-Beam Diffraction Technique

Willis, et al. (1975) have developed a technique to measure film thickness by laser-beam diffraction. Their approach is based on the fact that a beam of light passing through a small gap is diffracted. The diffraction patterns obtained are a series of light and dark bands. For dry gaps and a monochromatic coherent light source, such as a laser beam, it can be shown that a simple relationship exists between gap thickness, the spacing between fringes in the resulting diffraction pattern, the distance between the gap and the screen displaying the diffraction pattern, and the wavelength of light from the laser. However, when lubricant is present in the gap, the resulting diffraction pattern becomes distorted by the oil film in the gap. From experiments conducted by Willis, et al. (1975) an empirical relationship was obtained between the actual fluid-film thickness and the film thickness calculated by diffraction

theory. Additional properties of the lubricant such as density, viscosity, and refractive index were also taken into account.

Interpreting diffraction patterns associated with fluid-film thicknesses of less than 7.62 μm becomes very difficult when using a relatively low power (1 mW) helium-neon laser. Diffraction pattern bandwidth is inversely proportional to film thickness, and for very large bandwidths or thin films the light intensity of the diffraction pattern is very much diluted. With present equipment this lower limit of film thickness measurement represents a serious disadvantage for this approach to the study of elastohydrodynamic films. This technique may, however, be of value in measuring film thickness in circular contacts in low-elastic-modulus elastohydrodynamic lubrication studies and in some conventional hydrodynamic lubrication situations.

10.2.4 Mechanical Techniques

Strain-Gauge Method

Meyer and Wilson (1971) have used a preloaded bearing and a strain gauge to measure elastohydrodynamic film thickness and wear in a ball bearing. This technique involves the mounting of a strain gauge on the outer ring of a bearing and measurement of the change in strain as the ball rolls around the race. The strain at any point on the outer race is the result of race

bending and axial tension. When the ball is directly under the strain gauge, the maximum tensile strain occurs; and when the ball is displaced by $360^\circ/2n$ from the gauge, where n is the number of balls, the minimum tensile strain occurs. The difference between maximum and minimum strain can be used to calculate the ball load, that is, the load imposed on each ball in a radial direction by the races. A theoretical curve is obtained that gives the relationship between the diametral clearance and the ball load. From Chapter 2 the diametral clearance is given as

$$P_d = d_o - d_i - 2d \tag{2.2}$$

The ball load is based on thin-ring bending theory, which assumes that the outer-ring radius is much larger than its thickness, and on Hertzian contact theory. If a low-viscosity lubricant is used and very slow speeds, such that the formation of effective lubricating films is prevented, the ball load and thus the initial diametral interference are obtained from the measured strain. At the desired speed and with the normal lubricant, elastohydrodynamic films are formed and the effective ball load and the effective diametral clearance can be determined again from the measured strain. The difference between the effective diametral clearance in the running bearing and the initial diametral clearance can be used to interpret the film thickness in an actual bearing.

This technique has promise for applications in rolling elliptical contacts because it gives a measurement of dynamic

elastohydrodynamically lubricated film thickness under operating conditions. A most important feature of the technique is that, unlike other procedures, it does not rely on a simulation of bearing operation.

Spring Dynamometer Method

Johnson and Roberts (1974) have used a spring dynamometer to study the variation of film thickness with load in elastohydrodynamically lubricated contacts. This technique uses changes in the dynamometer spring compression as a measure of the film thickness. The spring dynamometer is used to measure the compressive load between two concentric, counterrotating flat plates nipped together and having equally spaced steel balls rolling between them. The plates are mounted on a central spindle through angular-contact ball bearings. A precision dial gauge is used to measure changes in displacement due to variation in the spring compression. As the plates rotate, an elastohydrodynamic film is developed between the plates and the rolling balls. This gives a relative displacement between the plates, which is detected as a change in load and an associated change in spring compression at the dynamometer.

The measured film thickness represents only the average film thickness in the conjunction. Inaccuracies in film thickness measurements with this technique are significant because it

is extremely difficult, if not impossible, to record variations in displacements of fractions of a micrometer, or a few micro-inches, under dynamic conditions by using mechanical components.

10.3 Comparison Between Theoretical and Experimental Film Thickness

Now that film thickness predictions have been developed theoretically in Chapters 8 and 9 and the various experimental techniques adopted for measuring film thickness have been described in the last section, the present discussion is primarily concerned with a comparison of predicted and measured film thicknesses.

The minimum- and central-film-thickness equations developed in Chapter 8 for fully flooded conjunctions are not only useful for design purposes, but they also provide a convenient means of assessing the influence of various parameters on the elastohydrodynamic film thickness. For the purpose of comparing theoretical film thicknesses with those found in actual elastohydrodynamic contacts, Table 10.1 was obtained from Kunz and Winer (1977). The experimental apparatus consisted of a steel ball rolling and sliding on a sapphire plate; this generated a circular conjunction, or an ellipticity parameter of unity. Measurements were made by using the technique of optical interferometry described earlier in this chapter. Table 10.1 shows the results

of both calculations and measurements for three lubricants in pure sliding, each under two different loads and three speeds. The notation H_{min} and H_c is used to denote the dimensionless film thickness calculated from equations (8.23) and (8.41), respectively. The measured minimum and central film thicknesses obtained from Kunz and Winer (1977) are denoted by H_{min} and H_c. Figures 10.8 and 10.9 show comparisons between the calculated and measured film thicknesses for the two loads noted in Table 10.1.

For the smaller load ($W = 0.1238 \times 10^{-6}$) the results shown in Figure 10.8 compare remarkably well if we bear in mind the difficulties associated with the experimental determination of such small quantities under arduous conditions and the error associated with the complex numerical evaluations of elastohydrodynamic conjunctions. The ratios between the central and minimum film thicknesses are similar for the calculations and the measurements, and the dependence of film thickness on speed thus appears to be well represented by equations (8.23) and (8.41).

For the larger load ($W = 0.9287 \times 10^{-6}$) the agreement shown in Figure 10.9 is not quite so good, with the theoretical predictions of film thickness being consistently larger than the measured values. This discrepancy is sometimes attributed to viscous heating, as discussed by Greenwood and Kauzlarich (1973), or to non-Newtonian behavior, as discussed by Moore

(1973). Viscous heating appears to enjoy the most support as a concept to account for the discrepancy. Since the measurements were made in a condition of pure sliding, thermal effects might well be significant, particularly at the larger load. The value of viscosity used in the calculations reported in Table 10.1 was that corresponding to the temperature of the lubricant bath. If thermal effects become important, the isothermal assumption used in deriving equations (8.23) and (8.41) is violated. But, although the value of the viscosity used in these expressions is necessarily somewhat arbitrary, there is evidence from previous studies of line or rectangular elastohydrodynamic conjunctions that the film thickness is determined by the effective viscosity in the inlet region. If this viscosity is known with reasonable accuracy, the predicted film thicknesses are quite reliable. In addition, at the more severe conditions imposed by the larger load, the lubricant may no longer behave as a Newtonian liquid. This would violate the assumptions used in deriving equations (8.23) and (8.41).

The results of Kunz and Winer (1977) presented in Table 10.1 and Figures 10.8 and 10.9 suggest that at large loads there is a more rapid change in lubricant film thickness than would be predicted by isothermal elastohydrodynamic theory for elliptical conjunctions as represented by equations (8.23) and (8.41). This view is supported by the experimental results based on the X-ray technique reported by Parker and Kannel (1971) and the

results of optical interferometry presented by Lee, et al. (1973). This observation, however, contradicts the results of Johnson and Roberts (1974), who used the spring dynamometer method described in the last section to estimate elastohydrodynamic film thickness. Johnson and Roberts found that in spite of the approximate nature of their method, the results indicated quite strongly that the elastohydrodynamic film thickness as predicted by equations (8.23) and (8.41) was maintained up to the highest contact pressures that are practical with ball bearing steels. Their results support the more precise measurements of Gentle and Cameron (1973) and extend the range of operating conditions to higher rolling speeds. The discrepancy between these investigations in regard to the influence of load on elastohydrodynamic film thickness has yet to be explained.

Another comparison between experimental findings and theoretical predictions can be based on the experimental results provided by Dalmaz and Godet (1978). They measured film thickness optically in a pure-sliding, circular-contact apparatus for different fire-resistant fluids. An example of the good correlation between the theoretical predictions based on the equations developed in Chapter 8 and these experimental results is shown in Figure 10.10. The agreement between the theoretical predictions and the experimentally determined variation of central film thickness with speed for mineral oil and water-glycol lubricants of similar viscosity is most encouraging. The ellip-

ticity parameter was unity and the applied load was 2.6 N for these experiments. Figure 10.10 also shows that for waterglycol the film thickness generated was barely one-third of that developed for mineral oil of similar viscosity. This drastic reduction in film thickness is attributed to the pressure viscosity coefficient of water-glycol, which is only about one-fifth that of mineral oil.

Two further and important comparisons between the theoretical film thickness equations developed in this text and experimental measurements of film thickness in elliptical elastohydrodynamic conjunctions were presented in the summer of 1980. In the first of these Koye and Winer (1980) presented experimental values of film thickness for ellipticity ratios ranging from 3.7 to 0.117, and Swingler (1980) provided remarkably consistent experimental results based on a new approach to optical interferometry.

Koye and Winer (1980) used optical interferometry to provide minimum film thicknesses between a steel crowned roller and a flat sapphire disc. The seven crowned rollers used in the experiments were machined from A-2 tool steel, hardened to a Rockwell hardness of R_c 60 and then sanded and polished to a surface roughness of less than 0.13 μm. The radius of the crown was determined by loading the disc against the sapphire disc, measuring the ellipticity ratio, and then deducing the value of

R_y from equation (3.28). The average value of r_x was 15.6 mm and the crown radii r_y varied from 116.2 to 0.56 mm.

The sapphire disc, which was optically flat to within an eighth of a wavelength of light, had a diameter of 88.9 mm, a thickness of 3.2 mm and a surface roughness of 0.00635 μm. The disc was coated with Inconel to give a partially reflective surface.

The lubricant was a naphthenic base mineral oil with a coefficient of viscosity of 0.093 N s/m^2 and a pressure-viscosity coefficient of 31.9 m^2/GN at 40° C. The pressure-viscosity properties of the lubricant and the effective elasticity of the crowned rollers and the sapphire disc yielded an average value of the dimensionless materials parameter G of 10,451. The dimensionless speeds U and loads W were varied by changing the rolling velocities and the applied loads such that

$$2.14\times10^{-11} < U < 8.90\times10^{-11}$$

$$0.038\times10^{-6} < W < 5.32\times10^{-6}$$

Some 63 film thickness measurements were attempted by means of optical interferometry, and 57 acceptable results were obtained. A statistical analysis of the results showed that the experimental values of minimum film thickness were about 23 percent greater than the corresponding predictions of the Hamrock and Dowson equation (8.23) for values of $k \geq 1$. The ratio of the experimental to theoretical minimum film thicknesses tended

to increase when k was less than unity, but the average value of the ratio over the full range of results was about 1.3. The mean difference between measured and predicted film thickness was only 0.17 μm, with the mean of the measured film thickness being 0.667 μm. Koye and Winer (1980) found that their results suggested that both dimensionless speed U and load W had a slightly more dominant influence on minimum film thickness than the theory indicated.

A summary of the results, in which the experimental dimensionless minimum film thicknesses are plotted against the theoretical predictions, is shown in Figure 10.11.

There are three significant features of the findings of this important experimental investigation:

(1) The theoretical minimum-film-thickness equation (8.23) tends to underestimate the actual minimum film thickness.

(2) The experimental findings suggest that the theoretical minimum-film-thickness formula (8.23) is just as valid for ellipticity ratios less than unity as it is for values of the ratio greater than unity.

The first conclusion appears to contradict the earlier findings of Kunz and Winer (1977), although it has to be said that the overall agreement between theory and experiment in this difficult field is encouraging. If the finding that the minimum-film-thickness formula tends to underestimate the actual film

thickness is confirmed, the theoretical predictions will at least possess the merit of being conservative.

Perhaps the most remarkable and valuable feature of this study is that it has confirmed the utility of the minimum-film-thickness formula at values of k considerably less than unity. This is well outside the range of ellipiticity ratios considered by Hamrock and Dowson in their numerical solutions to the elastohydrodynamic problem, and it engenders confidence in the application of the film thickness equation to machine elements that normally produce a long, elliptical contact in the direction of motion. This field of applications includes the roller-flange conjunction in axially loaded roller bearings, Novikov gear contacts, and certain situations involving micro-elastohydrodynamic action on surface asperities.

Swingler (1980) developed a most interesting alternative optical technique for the measurement of elastohydrodynamic film thickness by taking advantage of an inherent weakness of optical interferometry involving rough surfaces. The contrast, or difference between the maximums and minimums of the intensity trace, gives a measure of the surface topography within the contact. If the intensity is continuously monitored, the intensity turning points also give an objective measure of film thickness, with the interval between consecutive turning points being $\lambda/4n$, where λ is the wavelength of light and n is the refractive index of the medium. Although the technique was primarily de-

veloped to monitor topographical changes in elastohydrodynamic contacts, it also provides an accurate measure of film thickness. This has now been achieved by Swingler in Professor Cameron's lubrication laboratory at Imperial College, London.

The change in film thickness was achieved by changing the rolling speed and the interval between successive turning points on a trace of intensity as a function of time corresponding to a change in film thickness of $\lambda/4n$. A particular advantage of this procedure is that the film thickness changes can be indentified accurately and without the problems of interpretation associated with the monitoring of fringes in conventional optical interferometry.

A four-disc machine in which load was applied hydrostatically was used for the experimental investigation, with the outer disc being made of steel and the inner disc of sapphire. The EN 30B steel discs had a nominal radius of 25.4 mm, a Vickers hardness of 330, a Poisson's ratio of 0.3, and a modulus of elasticity of 207 GN/m^2.

The sapphire disc was made from a single crystal and had a nominal radius of 12.7 mm, a refractive index of 1.765, a Poisson's ratio of 0.265, and a modulus of elasticity of 432 GN/m^2. Two paraffinic mineral oils with coefficients of viscosity of 0.0792 N s/m^2 at 37.8° C (0.79 poise at 100° F) and pressure-viscosity coefficients α given by the following expression were used in the experiments:

$$\alpha = (2.710 - 0.0111\ T_m)x10^{-8}\ m^2/N$$

where T_m is the temperature in degrees C.

The refractive index n^* of the lubricants was 1.4876 at 20^0 C, and the relationship between n^* and the temperature T_m in degrees Celsius was written as

$$n^* = 1.495(1 - 0.000235\ T_m)$$

In the pure rolling experiments the discs were accelerated from zero to a maximum surface speed of about 2 m/s in a period of 30 s and then decelerated until the speed returned to zero in a similar time. The contact condition at zero speed provided a sound datum for film thickness measurements.

The variation of measured central film thickness with the dimensionless speed U is compared with the predictions of the Hamrock and Dowson equation (8.41) in Figure 10.12. Loads corresponding to peak Hertzian pressures of 1.43 and 1.89 GN/m^2 were employed, and the ellipticity ratio was close to 20. These contact pressures are quite severe and certainly representative of the practical conditions encountered within rolling-element bearings.

The consistency of the experimental readings during both accelerating and decelerating conditions is quite remarkable. Furthermore the agreement between the experimental values and the predictions of equation (8.41) is excellent at a peak contact pressure of 1.43 GN/m^2, and the theoretical predictions

exceed the experimental values by only 10 percent at the higher peak contact pressure of 1.89 GN/m^2.

It appears that measurements of intensity changes in optical interferometry offer a new and remarkable system for the measurement of elastohydrodynamic film thickness. Furthermore the close agreement between theory and experiment offers considerable support for the validity of equation (8.41). It is particularly important to note that the values of peak contact pressures considered in these experiments far exceed those adopted in the numerical solutions on which equation (8.41) is based.

The indications from the experimental studies of Koye and Winer (1980) and Swingler (1980) that the film thickness equations developed in this text can be applied in situations where the ellipticity ratio and peak Hertzian contact stresses fall well outside the original range of parameters considered in the numerical work is particularly important.

Various theoretical predictions are compared with the experimental results of Archard and Kirk (1964) in Figure 10.13. These results are presented in a form that indicates the influence of side leakage on film thickness in elliptical contacts by plotting a film reduction factor $H_{min}/H_{min,r}$ against the effective radius ratio R_x/R_y. The factor $H_{min}/H_{min,r}$ is defined as the ratio of the minimum film thickness achieved in an elliptical contact to that achieved in a rectangular contact formed between two cylinders in nominal line contact. The theo-

retical results of Archard and Cowking (1965-66), Cheng (1970), and Hamrock and Dowson (1977a), along with the theoretical solution for rigid solids by Kapitza (1955), are presented in this figure. Archard and Cowking (1965-66) adopted a theoretical approach for elliptical contacts similar to that used by Grubin (1949) for a rectangular-contact condition. The Hertzian contact zone is assumed to form a parallel film region, and the generation of high pressure in the approach to the Hertzian zone is considered.

Cheng (1970) solved the coupled system of equations separately by first calculating the deformations from the Hertzian equations. He then applied the Reynolds equation to this geometry. He did not consider a change in the lubricant density and assumed an exponential law for the viscosity change due to pressure. Hamrock and Dowson (1977a) developed a procedure for the numerical solution of the complete isothermal elastohydrodynamic lubrication problem for elliptical contacts, which is also presented in Chapter 7.

For $0.1 < R_x/R_y < 1$ the Archard and Cowking (1965-66) and Hamrock and Dowson (1977a) predictions are in close agreement and both overestimate the reduction in film thickness evident in the experimental results of Archard and Kirk (1964). For $1 < R_x/R_y < 10$ the Hamrock and Dowson (1977a) predictions of film thickness exceed and gradually diverge from those of Archard and Cowking (1965-66). They are also in better

agreement with the experimental results of Archard and Kirk (1964). Cheng's (1970) theoretical predictions are optimistic and differ significantly from the experimental data. Kapitza's (1955) rigid-contact theory is also optimistic about the reduction in film thickness compared with the experimental results, but it is in somewhat closer agreement with experiment than the Cheng (1970) results. These comparisons between theory and experiment offer reasonable grounds for confidence in the predictions of the complete three-dimensional elastohydrodynamic lubrication theory for elliptical contacts presented in Chapter 7.

Attention has been focused on the minimum and central film thicknesses in the conjunction, but there is also some interest in the film thickness throughout the conjunction. When the amount of lubricant in the inlet region is limited, the contact may suffer from the effects of lubricant starvation. The application of optical interferometry provides such details, and an example of the interference pattern for a starved conjunction, which was kindly supplied by Sanborn from the work he reported in 1969, is shown in Figure 10.14. This technique produces information of great clarity and beauty. The shapes of the lubricated conjunction in a starved condition revealed by the experimental result shown in Figure 10.14 compare quite well in qualitative terms with the theoretical results shown in Chapter 9.

10.4 Pressure Measurements

The pressure distribution within small elastohydrodynamic conjunctions has been revealed in a series of carefully conducted experiments involving the use of fine strips of manganin deposited on the insulated surfaces of discs in a disc machine. Manganin is an alloy of copper, nickel, and manganese whose resistance is influenced by pressure. Hence changes in electrical resistance can be interpreted as changes in pressure. The technique was developed by Kannel, et al. (1964), extended by Cheng and Orcutt (1965-66), and used to reveal the presence of attenuated pressure spikes in an impressive study by Hamilton and Moore (1971).

Theoretical and experimental pressure distributions are compared for a range of speeds at a constant load in Figure 10.15 and for a range of loads at a constant speed in Figure 10.16, as recorded by Hamilton and Moore (1971). A rectangular contact was assumed, and a theoretical procedure simulating that used by Dowson and Higginson (1959) provided the theoretical solutions shown in these figures. The theoretical results are represented by the chain-dotted line, the experimental results by the solid line, and the Hertzian pressure distribution by the dashed line. In both figures the results are presented with pressure in giganewtons per square millimeter.

In Figure 10.15 the theoretical and experimental pressure distributions are shown for speeds of 5.18, 2.69, and 1.3 m/s at a constant load per unit length of 100.3 kN/m. There is a broad level of agreement between the theoretical and experimental results, with the pressure peaks occurring essentially in the predicted position and moving forward toward the inlet in the expected manner (also see Figure 8.6) as the speed increases. The main discrepancy concerns the height of the pressure spike. The height of the experimental pressure spike hardly changes with speed and remains at all times considerably below the theoretical value.

Figure 10.16 shows the theoretical and experimental pressure distributions for loads per unit length of 100.3, 54.2, and 31.1 kN/m, at a constant speed of 1.3 m/s. Variations in load have a much greater effect on the shape of the pressure distribution than does the variation in speed shown in Figure 10.15. Again, the general agreement between the results is good, the main discrepancy being in the height of the pressure spike. At the lowest load, where a spike is not predicted theoretically, the agreement is extremely good. The main conclusion to be drawn from the experimental results of Hamilton and Moore (1971) is that although there is indeed a pressure spike in the outlet region in the position demanded by theory, it is much smaller than predicted.

10.5 Temperature Measurements

Temperature within, or adjacent to, elastohydrodynamic contacts has been recorded by embedded and trailing thermocouples and by thin films of platinum (Cheng and Orcutt, 1966) and nickel (Hamilton and Moore, 1971) on a glass disc. Although the probes were small, they accounted for 8 to 10 percent of the film thickness under typical operating conditions. The conditions were limited in severity because of the glass surface and the fragile nature of the gauges.

A noncontacting technique based on infrared measurements was developed by Turchina, et al. (1974) and further developed by Ausherman, et al. (1976) and Nagaraj, et al. (1977). It has the advantages that it does not interfere in any way with the operation of the elastohydrodynamic conjunction and that it can be used under conditions of contact severity comparable to those encountered in real engineering applications. The test apparatus used by these authors is shown diagrammatically in Figure 10.17. The sliding elastohydrodynamic conjunction was formed by using a 31.8-mm-diameter rotating chromium steel (52100) ball loaded against a sapphire flat. The infrared radiation emitted from the conjunction was measured with a radiometric detector having a spot size resolution of 38 μm. A temperature-controlled lubricant supply system was used to provide the conjunction with fluid at constant temperature. With this

technique each filter permits a specific bandwidth of infrared radiation to pass on to the detector. One filter covers a bandwidth in which the fluid is transparent, does not emit, and allows the ball temperature to be determined. The second filter covers the carbon-hydrogen emission band of the test lubricant and, after calibration of the system to include the effects of temperature and lubricant film thickness on emissivity, permits the reliable determination of the oil film temperature. Ausherman, et al. (1976) used this technique to generate the contours shown in Figures 10.18 and 10.19 for the ball surface T_b and average lubricant temperatures T_f, respectively. The ball surface temperature is shown in Figure 10.18 as a function of location in the elastohydrodynamic conjunction for a sliding speed of 1.4 m/s and a load of 67 N, which give a peak stress of 1.05 GN/m^2. Because of symmetry in the contact, only one-half of the map is shown. Isotherms are shown in increments of 10 degrees Celsius along with the boundary of the Hertzian contact zone. For a reservoir temperature of 40^o C, the ball temperature increases to a maximum of 117^o C at a point on the line of symmetry downstream of the conjunction center.

A similar map for the lubricant temperature under the same operating conditions is shown in Figure 10.19. However, in this case the lubricant was heated to over 120^o C before it entered the contact zone. Unlike the well-behaved distribution of ball

temperature shown in Figure 10.18, the fluid temperature shown in Figure 10.19 varies dramatically, indicating the presence of local "hot" spots. Although one of these locations was near the point of maximum ball surface temperature, extreme temperatures were also found at the sides of the contact near the film constriction. The film thickness at this point was approximately 0.05 μm.

The revelation of such large temperatures within such a small conjunction by the direct use of infrared techniques contributed greatly to the understanding of the phenomenon of elastohydrodynamic lubrication in sliding contacts.

Up to the middle of this century the major problem in relation to the lubrication of highly stressed machine elements such as gears and ball bearings had been to understand how a coherent film of lubricant could be developed under such arduous conditions. However, by the end of the 1960's, when the beautiful feat of nature known as elastohydrodynamic lubrication had been revealed to scientists and engineers, it was difficult to see how lubricant films, once formed, could ever fail. The situation revealed by infrared techniques showed that the temperature required for chemical reactions and lubricant deterioration could, in fact, occur in the complex situation within elastohydrodynamic films.

Figures 10.20 and 10.21 are also drawn from results obtained by Ausherman, et al. (1976). Figure 10.20 shows that, for Hertzian stress levels of 0.52 to 2.0 GN/m^2, the logarithm

of ball surface temperature varies linearly with the logarithm of speed. In some cases, however, there is a particular sliding speed where the slope of the line changes significantly. Note that the most significant change in slope occurs for the higher pressure cases, where the film thickness is relatively small. The parameter Λ was defined in equation (3.114) as the ratio of film thickness to composite surface roughness. The value of Λ is greater than 2 for all speeds and stress levels shown in Figure 10.20 except for the 2.0 GN/m^2 stress case, where $1 < \Lambda < 2$. The change in temperature rise with sliding speed might then be explained by a transition from significant asperity interaction at the lower speeds to little interaction at the higher speeds.

Figure 10.21, also from Ausherman, et al. (1976), shows the surface temperature rise above ambient at the center of the contact plotted as a function of the maximum Hertzian pressure for three different sliding speeds. In all three cases the ratio of film thickness to composite surface roughness was greater than unity. It is clear that the ball surface temperature is strongly influenced by the Hertzian contact pressure.

Nagaraj, et al. (1977) used the infrared technique discussed earlier in this section and found the ball surface temperature rise ΔT, defined as the ball surface temperature minus the bulk oil temperature, at the center of the elastohydrodynamic contact to be a function of the peak Hertzian pressure

p_{max} and the sliding velocity v, or $\Delta T = f(p_{max}v)$. The relationship between ball surface temperature rise and speed exhibits two distinct characteristics determined by speed. At low speeds the temperature rises more quickly with sliding speed than at high speeds, with the transition velocity v^* being a function of the Hertzian pressure. The magnitude of v^* can be described by

$$v^* = 1.564\ p_{max}^{-3.22} \tag{10.1}$$

The following results of Nagaraj, et al. (1977) were obtained after a multiple regression analysis of the experimental data:

$$\text{For } v < v^* \qquad \Delta T = 46.99\ p_{max}^{2.02} v^{0.53} \tag{10.2}$$

$$\text{For } v \geq v^* \qquad \Delta T = 53.52\ p_{max}^{1.34} v^{0.34} \tag{10.3}$$

It is clear from these relationships that the ball surface temperature is a much stronger function of contact pressure than of sliding velocity.

Except for the present section it has been assumed throughout this text that the lubricant properties are those at the lubricant temperature in the inlet zone and that the system is isothermal. The inlet zone lubricant temperature can be, and frequently is, higher than the bulk lubricant temperature. This increase in lubricant temperature in the inlet zone is mainly attributable to viscous shearing, often accomplished by reverse flow. The viscous heating affects the film thickness and be-

comes important as the surface speeds increase and can, with some assumptions, be analyzed. One approach to estimating the thermal film reduction resulting from viscous heating has been proposed by Cheng (1967). Cheng gives a thermal reduction factor ϕ_T that can be multiplied by the isothermal film thickness presented in Chapters 8 and 9 to give a better estimate of the actual film thickness ($h^* = h\phi_T$). The thermal correction factor is a weak function of the load and materials parameters. As a first approximation Figure 10.22 can be used to determine the correction factor for line or rectangular contacts. In Figure 10.22 the thermal loading parameter Q_m is defined as

$$Q_m = \frac{\eta_0 u^2 \delta^*}{k_f} \tag{10.4}$$

where

η_0 = lubricant viscosity at atmospheric pressure and the inlet surface temperature, N s/m^2

u = the average surface velocity, $(u_a + u_b)/2$, m/s

δ^* = lubricant viscosity temperature coefficient, C^{-1}

k_f = lubricant thermal conductivity, N/s K

An inlet heating analysis does not exist at present for elliptical contacts but Figure 10.22 can be used to give some indication of the importance of inlet shear heating for elliptical-contact problems.

10.6 Traction Measurements

The lubricant in an elastohydrodynamic conjunction experiences rapid and very large pressure variations, a short transit time, possibly large temperature changes, and (particularly in sliding contacts) high shear rates. The great severity of these conditions has caused the normal assumption of Newtonian behavior adopted in the analysis to be questioned. The assumption appears to be acceptable as far as film thickness prediction is concerned, as demonstrated by the agreement between theory and experiment presented earlier in this chapter. However, it may be unrealistic when details of the pressure and temperature distribution are considered and is certainly inadequate when traction has to be considered.

The determination of the traction in elastohydrodynamic contacts is of primary importance in understanding many lubricated mechanisms. Traction is defined as the force generated in the contact that resists relative motion of the bearing surfaces. This is directly related to the power loss in such mechanical components as gears, cams, and rolling-element bearings. Traction is thus important in relation to energy losses and thermal effects in bearings and gears and vital to the functioning of a number of variable-speed drives. Traction studies are also motivated by the need to predict the onset of sliding in rolling-element bearings.

Studies of the shear properties of a lubricant during short periods of time ($\sim 10^{-3}$ s) when it is passing through a high-pressure ($\sim 10^{9}$ Pa) contact have usually been carried out on a disc machine in which the discs rotate with peripheral speeds u_a and u_b. The discs are pressed together by a normal force F, which flattens the discs elastically in their contact zone according to Hertzian theory. The mean rolling speed or entraining velocity $u = (u_a + u_b)/2$ draws lubricant into the nip between the discs and generates an oil film of approximately uniform film thickness h. The sliding speed $\Delta u = u_a - u_b$ shears this fluid and gives rise to a tangential (traction) force $\tilde{T}$. In a typical experiment the load and rolling speed and hence the pressure and film thickness are kept constant. The variation of traction force with increasing sliding speed is measured. This gives rise to the familiar "traction curve" shown in Figure 10.23, which was obtained by Johnson and Cameron (1967).

Since the surface area $\tilde{A}$ of the film and its thickness remain essentially constant for each experiment, the traction curve shows the variation of mean shear stress in the film $\tilde{\tau} = \tilde{T}/\tilde{A}$ with shear rate $\dot{\gamma} = \Delta u/h$. In general the curves display three regions: (1) a linear region in which τ is proportional to $\dot{\gamma}$ as for a Newtonian fluid; (2) a nonlinear, shear-thinning region; and (3) at high pressures and high shear rates a region where the stress falls with increasing shear rate.

From Figure 10.23 we see that pressure is a dominant parameter. At high pressure the linear region is restricted to extremely low sliding speeds, and traction is dominated by the nonlinear behavior of the lubricant. It also appears that the initial linear region of the traction curve might owe as much to the elastic properties of the lubricant as it does to its viscous properties.

Various hypotheses have been advanced to account for the nonlinear region in Figure 10.23. A good review of the subject was presented by Johnson and Tevaarwerk (1977). From this review and recent developments the variaous hypotheses used to account for the nonlinear region of the traction curve can be summarized as follows:

(1) Following the analysis of Fromm (1948), Dyson (1970) suggested that the nonlinear part of the traction curve arises from the fact that a viscoelastic material whose constitutive equation is intrinsically linear exhibits an apparent decrease in viscosity in steady, continuous shear when the strains become large.

(2) An alternative explanation is that at high pressures the relationship between stress and strain rate for the fluid is nonlinear. Such a model of fluid behavior was examined by Bell, et al. (1964); by Hirst and Moore (1974), who used a "sinh" relationship between strain rate and stress; and by Trachman and Cheng (1972), who used a hyperbolic relationship.

(3) The fact that the mean shear stress in an elastohydrodynamically lubricated film reaches a maximum value that rarely exceeds 10 percent of the mean pressure in the film led Smith (1962) to propose that the film was shearing as a plastic solid rather than as a viscous liquid. This view found support in the work of Plint (1967) and Johnson and Cameron (1967).

(4) Attention was drawn to a further complication in the process by Fein (1968) and developed by Harrison and Trachman (1972). They suggested that the fluid, in its brief passage through the contact, would not have time to respond completely to the high imposed pressure. Thus the values of density, viscosity, and shear modulus in the film must be lower than the equilibrium values under a steadily sustained pressure.

(5) Johnson and Tevaarwerk (1977) used a simple, nonlinear constitutive equation for elastohydrodynamic films that appears to account in a broad way for the observed shear behavior and reconciles some of the apparently conflicting hypotheses. The equation that they proposed is capable of describing linear elastic or linear viscous, nonlinear viscous, and (in the limit) elastic-plastic behavior.

(6) Another nonlinear viscous and plastic model was introduced recently by Bair and Winer (1979). In many respects the Bair and Winer model is similar to the Johnson and Tevaarwerk (1977) model except that the rheological constants in the former model were obtained from tests that were totally

independent of any data from the elastohydrodynamic lubricated contact itself.

The Johnson and Tevaarwerk (1977) model is expressed as

$$\dot{\gamma} = \dot{\gamma}_e + \dot{\gamma}_v = \frac{1}{G^*}\frac{d\tilde{\tau}}{dt} + \frac{\tilde{\tau}\tilde{\tau}_0}{\tilde{\tau}_e \eta}\sinh\left(\frac{\tilde{\tau}_e}{\tilde{\tau}_0}\right) \qquad (10.5)$$

where

$\dot{\gamma}$ = total strain rate, s^{-1}

$\dot{\gamma}_e$ = elastic strain rate, s^{-1}

$\dot{\gamma}_v$ = viscous strain rate, s^{-1}

$\tilde{\tau}$ = shear stress, N/m^2

G^* = fluid shear modulus, N/m^2

$\tilde{\tau}_e$ = equivalent stress, N/m^2

$\tilde{\tau}_0$ = representative stress, a measure of the stress about which the fluid becomes appreciably nonlinear, N/m^2

η = lubricant viscosity, $N\ s/m^2$

For normal operating conditions this equation has three fluid parameters - G^*, η, and $\tilde{\tau}_0$ - each of which can be determined from traction curves. In order to integrate equation (10.5) to find the shear stress, it is necessary to know the variations of the fluid properties η, G^*, and $\tilde{\tau}_0$ throughout the film. These parameters depend on temperature and pressure and possibly on the rate of pressure application. Johnson and Tevaarwerk (1977) chose to allow the parameters η, G^*, and $\tilde{\tau}_0$ to be uniform throughout the film and to adopt values depending on the average pressure and temperature in the film and on the average

time for the oil to pass through the contact. With this approximation it is a straightforward matter to integrate equation (10.5) to obtain the theoretical isothermal curves shown in Figure 10.24. A circular contact area ($k = 1$) of radius a was considered. The shape of the traction curve is a function of the Deborah number $De = \eta U/G^*a$, which is the ratio of the fluid relaxation time η/G^* to the time of fluid passage through the contact zone a/U.

For small Deborah numbers, associated with low-viscosity fluids and low pressures, elastic effects are negligible and the traction curve follows the viscous sinh law - being linear (Newtonian) at small strain rates and becoming increasingly nonlinear at high strain rates.

At medium to large Deborah numbers, brought about by a highly pressure-sensitive fluid or by high contact pressures, the response at small strain rates is linear and elastic. With the particular nondimensional variables plotted in Figure 10.24 the elastic response follows a single line for all values of De and is given by

$$\frac{\tilde{T}}{\pi a^2 \tilde{\tau}_0} = \frac{8G^*\dot{\gamma} a}{3\pi U \tilde{\tau}_0} = \frac{8G^* a\, \Delta U}{3\pi U \tilde{\tau}_0} \qquad (10.6)$$

This is the elastic region revealed by the experiments of Johnson and Roberts (1974). From equation (10.6) the traction force can be written as

$$\tilde{T} = \frac{8G^* a^3\, \Delta U}{3Uh} \qquad (10.7)$$

It can be seen from Figure 10.4 that, for high Deborah numbers at small strain rates, the behavior is linear and elastic and that a rapid transition leads to a very "flat" curve at high strain rates. This shape strongly suggests that the lubricant is behaving like an elastic-plastic solid. Thus the Johnson and Tevaarwerk (1977) constitutive law equation (10.5) predicts traction curves (Figure 10.24) that reflect the observed behavior of elastohydrodynamic conjunctions subjected to shear over a complete range of conditions. Depending on the Deborah number and the stress level the shear behavior may be linear viscous (Newtonian), nonlinear viscous, linear elastic, or elastic-plastic.

The Bair and Winer (1979) model can be written in dimensionless form as

$$\dot{\gamma} = \dot{\gamma}_e + \dot{\gamma}_v = \frac{1}{G^*}\frac{d\tilde{\tau}}{dt} + \frac{\tilde{\tau}_L}{\eta}\tanh^{-1}\left(\frac{\tilde{\tau}}{\tilde{\tau}_L}\right) \qquad (10.8)$$

where $\tilde{\tau}_L$ is the limiting yield shear stress. From equation (10.8) it is seen that the three primary physical properties required to use the model are the low shear stress viscosity η, the limiting elastic shear modulus G^*, and the limiting shear stress $\tilde{\tau}_L$, all functions of pressure and temperature.

The difference in the Bair and Winer (1979) model (equation (10.8)) and the Johnson and Tevaarwerk (1977) model (equation (10.5)) occurs in the viscous shear rate expression $\dot{\gamma}_v$. If $\tilde{\tau}_L$ is made to be equal to $\tilde{\tau}\tilde{\tau}_0/\tilde{\tau}_e$ and the inverse hyperbolic tangent is replaced with the hyperbolic sine, the Bair and

Winer model would agree exactly with the Johnson and Tevaarwerk model. The following series points out the differences between these models:

$$\tilde{\tau}_L \tanh^{-1}\left(\frac{\tilde{\tau}}{\tilde{\tau}_L}\right) = \tilde{\tau}\left[1 + \frac{1}{3}\left(\frac{\tilde{\tau}}{\tilde{\tau}_L}\right)^2 + \frac{1}{5}\left(\frac{\tilde{\tau}}{\tilde{\tau}_L}\right)^4 + \cdots\right] \quad (10.9)$$

$$\tilde{\tau}_L \sinh\left(\frac{\tilde{\tau}}{\tilde{\tau}_L}\right) = \tilde{\tau}\left[1 + \frac{1}{3!}\left(\frac{\tilde{\tau}}{\tilde{\tau}_L}\right)^2 + \frac{1}{5!}\left(\frac{\tilde{\tau}}{\tilde{\tau}_L}\right)^4 + \cdots\right] \quad (10.10)$$

Making use of equations (10.9) and (10.10) for very large values of limiting shear stress (small values of $\tilde{\tau}/\tilde{\tau}_L$) reduces equations (10.8) and (10.5) to the Maxwell, or visco-elastic, model

$$\dot{\gamma} = \frac{1}{G^*}\frac{d\tilde{\tau}}{dt} + \frac{\tilde{\tau}}{\eta} \quad (10.11)$$

If a constant stress is applied at $t = 0$ equation (10.11) becomes

$$\gamma = \frac{\tilde{\tau}}{G^*} + \frac{\tilde{\tau}_t}{\eta} \quad (10.12)$$

This results in an instantaneous elastic strain $\tilde{\tau}/G^*$ and a time-dependent viscous strain $\tilde{\tau}_t/\eta$. The elastic and viscous strains are equal when

$$t = \frac{\eta}{G^*} = \text{Maxwell relaxation time} \quad (10.13)$$

If the material is given an initial strain γ_0 that is maintained constant, the initial stress will be $\tilde{\tau}_0 = G^*\gamma_0$. At some time t the stress is given as

$$\tilde{\tau} = G^*\gamma_{0e}^{-G^*t/\eta} \tag{10.14}$$

since $\gamma = 0$ and $\dot{\tilde{\tau}} + \tilde{\tau}G^*/\eta = 0$. If the time taken for the fluid to flow through an elastohydrodynamic contact is of the same order as the relaxation time, then elastic deformation will be important and a Maxwell or viscoelastic fluid should be assumed.

For large Maxwell relaxation times as compared with the time taken for the fluid to flow through the contact, the viscous strain rate dominates the elastic strain rate and equation (10.8) reduces to a representation for a Newtonian, or viscous, fluid model, where

$$\tilde{\tau} = \eta\dot{\gamma} \tag{10.15}$$

At the other extreme the limiting case of a viscoplastic fluid results from a small Maxwell relaxation time as compared with the time taken for the fluid to flow through the contact. For this condition the Bair and Winer model (equation (10.8)) takes on the nonlinear viscous form of

$$\dot{\gamma} = \dot{\gamma}_v = \frac{\tilde{\tau}_L}{\eta} \tanh^{-1}\left(\frac{\tilde{\tau}}{\tilde{\tau}_L}\right) \tag{10.16}$$

where

$$\eta = \eta_0 e^{\alpha p}$$

$$\tilde{\tau}_L = \tilde{\tau}_{L_0} + mp$$

m = slope of limiting shear stress-pressure relation

$\tilde{\tau}_{L_0}$ = zero-pressure value of limiting shear stress

The theoretical film thickness in an elastohydrodynamically lubricated contact determined by assuming that the lubricant is a Newtonian fluid agrees well with experimental predictions, as pointed out in Section 10.3. However, the prediction of surface traction based on the assumption that the lubricant is a Newtonian fluid does not accord well with experiments, so that either viscoelastic or viscoplastic fluid models have to be used depending on the value of the Maxwell relaxation time.

10.7 Closure

In this chapter various experimental studies of elastohydrodynamic lubrication have been reviewed. The various types of machines used in these investigations - such as the disc, two- and four-ball, crossed-cylinders, and crossed-axes rolling disc machines - have been described. The measurement of the most important parameters - such as film shape, film thickness, pressure, temperature, and traction - has been considered. Determination of the film thickness is generally the most important of these effects since it dictates the extent to which the asperities on opposing surfaces can come into contact and thus has a direct bearing on wear and fatigue failure of the contacting surfaces. Several different techniques for measuring film thickness have been described - including electrical resistance, capacitance, X-ray, optical interferometry, laser beam diffrac-

tion, strain gauge, and spring dynamometer methods. An attempt has been made to describe the basic concepts and limitations of each of these techniques. These various methods have been used by individual researchers, but there is no universally acceptable technique for measuring elastohydrodynamic film thickness. Capacitance methods have provided most of the reliable data for nominal line or rectangular conjunctions, but optical interferometry has proved to be the most effective procedure for elliptical contacts. Optical interferometry has the great advantage that it reveals not only the film thickness, but also details of the film shape over the complete area of the conjunction. Theoretical film thickness solutions were developed in Chapters 8 and 9, and the various experimental techniques available for measuring this important parameter have been described early in this chapter. This has been followed by a comparison of theoretical and experimental findings from various sources, and a pleasing agreement between the two has been noted. Attention has also been focused on experimental studies of other important aspects of elastohydrodynamic lubrication - such as pressure distribution, the temperature rise on the surface of the solids and within the lubricant, and traction.

Many of the essential features of elastohydrodynamic elliptical contacts have now been revealed by careful and ingenious experimental studies. A number of these features, particularly film shape and thickness, have also been revealed by theoretical

analysis. The overall agreement between theory and experiment suggests that the equations developed in Chapters 8 and 9 can be used with reasonable confidence to analyze many of the important, highly stressed, lubricated machine elements that are present in elliptical contacts.

SYMBOLS

A	constant used in equation (3.113)
$A^*, B^*, C^*, D^*, L^*, M^*$	relaxation coefficients
A_v	drag area of ball, m^2
a	semimajor axis of contact ellipse, m
$\bar{a}$	$a/2\bar{m}$
B	total conformity of bearing
b	semiminor axis of contact ellipse, m
$\bar{b}$	$b/2\bar{m}$
C	dynamic load capacity, N
C_v	drag coefficient
$C_1,\ldots,C_8$	constants
c	19,609 N/cm^2 (28,440 lbf/in^2)
$\bar{c}$	number of equal divisions of semimajor axis
D	distance between race curvature centers, m
$\tilde{D}$	material factor
$\bar{D}$	defined by equation (5.63)
De	Deborah number
d	ball diameter, m
$\bar{d}$	number of divisions in semiminor axis
d_a	overall diameter of bearing (Figure 2.13), m
d_b	bore diameter, m
d_e	pitch diameter, m
d'_e	pitch diameter after dynamic effects have acted on ball, m
d_i	inner-race diameter, m
d_o	outer-race diameter, m

E	modulus of elasticity, N/m^2
E'	effective elastic modulus, $2\Big/\left(\frac{1-\nu_a^2}{E_a}+\frac{1-\nu_b^2}{E_b}\right)$, N/m^2
E_a	internal energy, m^2/s^2
$\tilde{E}$	processing factor
E_1	$[(\tilde{H}_{min} - H_{min})/H_{min}] \times 100$
$\mathscr{E}$	elliptic integral of second kind with modulus $(1 - 1/k^2)^{1/2}$
$\bar{\mathscr{E}}$	approximate elliptic integral of second kind
e	dispersion exponent
F	normal applied load, N
F^*	normal applied load per unit length, N/m
$\tilde{F}$	lubrication factor
$\bar{F}$	integrated normal applied load, N
F_c	centrifugal force, N
F_{max}	maximum normal applied load (at $\psi = 0$), N
F_r	applied radial load, N
F_t	applied thrust load, N
F_ψ	normal applied load at angle ψ, N
$\mathscr{F}$	elliptic integral of first kind with modulus $(1 - 1/k^2)^{1/2}$
$\bar{\mathscr{F}}$	approximate elliptic integral of first kind
f	race conformity ratio
f_b	rms surface finish of ball, m
f_r	rms surface finish of race, m
G	dimensionless materials parameter, αE
G^*	fluid shear modulus, N/m^2
$\tilde{G}$	hardness factor
g	gravitational constant, m/s^2

g_E	dimensionless elasticity parameter, $W^{8/3}/U^2$
g_V	dimensionless viscosity parameter, GW^3/U^2
H	dimensionless film thickness, h/R_x
$\hat{H}$	dimensionless film thickness, $H(W/U)^2 = F^2h/u^2\eta_0^2R_x^3$
H_c	dimensionless central film thickness, h_c/R_x
$H_{c,s}$	dimensionless central film thickness for starved lubrication condition
H_f	frictional heat, N m/s
H_{min}	dimensionless minimum film thickness obtained from EHL elliptical-contact theory
$H_{min,r}$	dimensionless minimum film thickness for a rectangular contact
$H_{min,s}$	dimensionless minimum film thickness for starved lubrication condition
$\tilde{H}_c$	dimensionless central film thickness obtained from least-squares fit of data
$\tilde{H}_{min}$	dimensionless minimum film thickness obtained from least-squares fit of data
$\bar{H}_c$	dimensionless central-film-thickness - speed parameter, $H_cU^{-0.5}$
$\bar{H}_{min}$	dimensionless minimum-film-thickness - speed parameter, $H_{min}U^{-0.5}$
$\bar{H}_0$	new estimate of constant in film thickness equation
h	film thickness, m
h_c	central film thickness, m
h_i	inlet film thickness, m

h_m	film thickness at point of maximum pressure, where dp/dx = 0, m
h_{min}	minimum film thickness, m
h_0	constant, m
I_d	diametral interference, m
I_p	ball mass moment of inertia, m N s^2
I_r	integral defined by equation (3.76)
I_t	integral defined by equation (3.75)
J	function of k defined by equation (3.8)
J*	mechanical equivalent of heat
$\bar{J}$	polar moment of inertia, m N s^2
K	load-deflection constant
k	ellipticity parameter, a/b
$\bar{k}$	approximate ellipticity parameter
$\tilde{k}$	thermal conductivity, N/s °C
k_f	lubricant thermal conductivity, N/s °C
L	fatigue life
L_a	adjusted fatigue life
L_t	reduced hydrodynamic lift, from equation (6.21)
$L_1,\ldots,L_4$	lengths defined in Figure 3.11, m
L_{10}	fatigue life where 90 percent of bearing population will endure
L_{50}	fatigue life where 50 percent of bearing population will endure
ℓ	bearing length, m
$\bar{\ell}$	constant used to determine width of side-leakage region
M	moment, Nm

M_g	gyroscopic moment, Nm
M_P	dimensionless load-speed parameter, $WU^{-0.75}$
M_s	torque required to produce spin, N m
m	mass of ball, N s^2/m
m*	dimensionless inlet distance at boundary between fully flooded and starved conditions
$\tilde{m}$	dimensionless inlet distance (Figures 7.1 and 9.1)
$\bar{m}$	number of divisions of semimajor or semiminor axis
m_W	dimensionless inlet distance boundary as obtained from Wedeven, et al. (1971)
N	rotational speed, rpm
n	number of balls
n*	refractive index
$\bar{n}$	constant used to determine length of outlet region
P	dimensionless pressure
P_D	dimensionless pressure difference
P_d	diametral clearance, m
P_e	free endplay, m
P_{Hz}	dimensionless Hertzian pressure, N/m^2
p	pressure, N/m^2
p_{max}	maximum pressure within contact, $3F/2\pi ab$, N/m^2
$p_{iv,as}$	isoviscous asymptotic pressure, N/m^2
Q	solution to homogeneous Reynolds equation
Q_m	thermal loading parameter
$\bar{Q}$	dimensionless mass flow rate per unit width, $q\eta_0/\rho_0 E' R^2$
q_f	reduced pressure parameter
q_x	volume flow rate per unit width in x direction, m^2/s

q_y	volume flow rate per unit width in y direction, m^2/s
R	curvature sum, m
R_a	arithmetical mean deviation defined in equation (4.1), m
R_c	operational hardness of bearing material
R_x	effective radius in x direction, m
R_y	effective radius in y direction, m
r	race curvature radius, m
r_{ax}, r_{bx}, r_{ay}, r_{by}	radii of curvature, m
r_c, ϕ_c, z	cylindrical polar coordinates
r_s, θ_s, ϕ_s	spherical polar coordinates
$\bar{r}$	defined in Figure 5.4
S	geometric separation, m
S*	geometric separation for line contact, m
S_0	empirical constant
s	shoulder height, m
T	τ_0/p_{max}
$\tilde{T}$	tangential (traction) force, N
T_m	temperature, °C
T_b^*	ball surface temperature, °C
T_f^*	average lubricant temperature, °C
ΔT^*	ball surface temperature rise, °C
T_1	$(\tau_0/p_{max})_{k=1}$
T_v	viscous drag force, N
t	time, s
t_a	auxiliary parameter
u_B	velocity of ball-race contact, m/s

u_c	velocity of ball center, m/s
U	dimensionless speed parameter, $\eta_0 u/E'R_x$
u	surface velocity in direction of motion, $(u_a + u_b)/2$, m/s
$\overline{u}$	number of stress cycles per revolution
Δu	sliding velocity, $u_a - u_b$, m/s
v	surface velocity in transverse direction, m/s
W	dimensionless load parameter, $F/E'R^2$
w	surface velocity in direction of film, m/s
X	dimensionless coordinate, x/R_x
Y	dimensionless coordinate, y/R_x
X_t, Y_t	dimensionless grouping from equation (6.14)
X_a, Y_a, Z_a	external forces, N
Z	constant defined by equation (3.48)
Z_1	viscosity pressure index, a dimensionless constant
$x, \tilde{x}, \bar{x}, \bar{x}_1$ $y, \tilde{y}, \bar{y}, \bar{y}_1$ $z, \tilde{z}, \bar{z}, \bar{z}_1$	coordinate system
α	pressure-viscosity coefficient of lubrication, m^2/N
α_a	radius ratio, R_y/R_x
β	contact angle, rad
β_f	free or initial contact angle, rad
β'	iterated value of contact angle, rad
Γ	curvature difference
γ	viscous dissipation, N/m^2 s
$\dot{\gamma}$	total strain rate, s^{-1}
$\dot{\gamma}_e$	elastic strain rate, s^{-1}
$\dot{\gamma}_v$	viscous strain rate, s^{-1}

γ_a	flow angle, deg
δ	total elastic deformation, m
δ^*	lubricant viscosity temperature coefficient, $^oC^{-1}$
δ_D	elastic deformation due to pressure difference, m
δ_r	radial displacement, m
δ_t	axial displacement, m
δ_x	displacement at some location x, m
$\overline{\delta}$	approximate elastic deformation, m
$\widetilde{\delta}$	elastic deformation of rectangular area, m
ϵ	coefficient of determination
ϵ_1	strain in axial direction
ϵ_2	strain in transverse direction
ζ	angle between ball rotational axis and bearing centerline (Figure 3.10)
ζ_a	probability of survival
η	absolute viscosity at gauge pressure, N s/m^2
$\overline{\eta}$	dimensionless viscosity, η/η_0
η_0	viscosity at atmospheric pressure, N s/m^2
η_∞	6.31×10^{-5} N s/m^2(0.0631 cP)
θ	angle used to define shoulder height
Λ	film parameter (ratio of film thickness to composite surface roughness)
λ	equals 1 for outer-race control and 0 for inner-race control
λ_a	second coefficient of viscosity
λ_b	Archard-Cowking side-leakage factor, $(1 + 2/3\ \alpha_a)^{-1}$
λ_c	relaxation factor

μ	coefficient of sliding friction
μ^*	$\overline{\rho}/\overline{\eta}$
ν	Poisson's ratio
ξ	divergence of velocity vector, $(\partial u/\partial x) + (\partial v/\partial y) + (\partial w/\partial z)$, s^{-1}
ρ	lubricant density, N s^2/m^4
$\overline{\rho}$	dimensionless density, ρ/ρ_0
ρ_0	density at atmospheric pressure, N s^2/m^4
σ	normal stress, N/m^2
σ_1	stress in axial direction, N/m^2
τ	shear stress, N/m^2
τ_0	maximum subsurface shear stress, N/m^2
$\tilde{\tau}$	shear stress, N/m^2
$\tilde{\tau}_e$	equivalent stress, N/m^2
$\tilde{\tau}_L$	limiting shear stress, N/m^2
Φ	ratio of depth of maximum shear stress to semiminor axis of contact ellipse
Φ^*	$PH^{3/2}$
Φ_1	$(\Phi)_{k=1}$
ϕ	auxiliary angle
ϕ_T	tnermal reduction factor
ψ	angular location
ψ_ℓ	limiting value of ψ
Ω_i	absolute angular velocity of inner race, rad/s
Ω_o	absolute angular velocity of outer race, rad/s
ω	angular velocity, rad/s
ω_B	angular velocity of ball-race contact, rad/s
ω_b	angular velocity of ball about its own center, rad/s

ω_c	angular velocity of ball around shaft center, rad/s
ω_s	ball spin rotational velocity, rad/s

Subscripts:

a	solid a
b	solid b
c	central
bc	ball center
IE	isoviscous-elastic regime
IR	isoviscous-rigid regime
i	inner race
K	Kapitza
min	minimum
n	iteration
o	outer race
PVE	piezoviscous-elastic regime
PVR	piezoviscous-rigid regime
r	for rectangular area
s	for starved conditions
x,y,z	coordinate system

Superscript:

$(\bar{\ })$	approximate

REFERENCES

Abbott, E. J. and Firestone, F. A. (1933) Specifying Surface Quality, Mech. Eng., 55, 569-572.

Agricola, G. (1556) De Re Metallica, Basel.

Aihara, S. and Dowson, D. (1979) "A Study of Film Thickness in Grease Lubricated Elastohydrodynamic Contacts," Proceedings of Fifth Leeds-Lyon Symposium on Tribology on 'Elastohydrodynamics and Related Topics', D. Dowson, C. M. Taylor, M. Godet, and D. Berthe, eds., Mechanical Engineering Publications, Ltd., 104-115.

Allan, R. K. (1945) Rolling Bearings, Sir Isaac Pitman & Sons, London.

Alsaad, M., Bair, S., Sanborn, D. M., and Winer, W. O. (1978) "Glass Transitions in Lubricants: Its Relation to Elastohydrodynamic Lubrication (EHD)," J. Lubr. Technol., 100(3), 404-417.

Amontons, G. (1699) "De la resistance caus'ee dans les machines," Memoires de l'Academie Royal, A, Chez Gerard Kuyper, Amsterdam, 1706, 257-282.

Anderson, W. J. (1978) "The Practical Impact of Elastohydrodynamic Lubrication," Proceedings of Fifth Leeds-Lyon Symposium on Tribology on 'Elastohydrodynamics and Related Topics,' D. Dowson, C. M. Taylor, M. Godet, and D. Berthe, eds., Mechanical Engineering Publications, Ltd., 217-226.

Anderson, W. J. and Zaretsky, E. V. (1968) "Rolling-Element Bearings." Mach. Des. (Bearing Reference Issue), 40(14), 22-39.

Anderson, W. J. and Zaretsky, E. V. (1973) "Rolling-Element Bearings - A Review of the State of the Art," Tribology Workshop sponsored by National Science Foundation, Atlanta, Ga., Oct. 19-20, 1972.

Archard, J. F. (1968) "Non-Dimensional Parameters in Isothermal Theories of Elastohydrodynamic Lubrication." J. Mech. Eng. Sci., 10(2), 165-167.

Archard, J. F. and Cowking, E. W. (1965-66) "Elastohydrodynamic Lubrication at Point Contacts," Proc. Inst. Mech. Eng., London, 180(3B), 47-56.

Archard, J. F. and Kirk, M. T. (1961) "Lubrication at Point Contacts" Proc. R. Soc. London, Ser. A, 261, 532-550.

Archard, J. F. and Kirk, M. T. (1964) "Film Thickness for a Range of Lubricants Under Severe Stress," J. Mech. Eng. Sci., 6, 101-102.

Ausherman, V. K., Nagaraj, H. S., Sanborn, D. M., and Winer, W. O. (1976) "Infrared Temperature Mapping in Elastohydrodynamic Lubrication," J. Lubr. Technol., 98(2), 236-243.

Baglin, K. P. and Archard, J. F. (1972) "An Analytic Solution of the Elastohydrodynamic Lubrication of Materials of Low Elastic Modulus," Proceedings of Second Symposium on Elastohydrodynamic Lubrication, Institution of Mechanical Engineers, London, 13.

Bair, S. and Winer, W. (1979) "Shear Strength Measurements of Lubricants at High Pressures," J. Lubr. Technol. 101(3), 251-257.

Bamberger, E. N. (1967) "The Effect of Ausforming on the Rolling Contact Fatigue Life of a Typical Bearing Steel," J. Lubr. Technol., 89(1), 63-75.

Bamberger, E. N. (1972) "The Thermomechanical Working of Electro-Slag Melted M-50 Bearing Steel," R72AEG290, General Electric Co., Cincinnati, Ohio.

Bamberger, E. N., Harris, T. A., Kacmarsky, W. M., Moyer, C. A., Parker, R. J., Sherlock, J. J., and Zaretsky, E. V. (1971) Life Adjustment Factors for Ball and Roller Bearings. American Society of Mechanical Engineers, New York.

Bamberger, E. N., Zaretsky, E. V., and Singer, H. (1976) "Endurance and Failure Characteristics of Main-Shaft Jet Engine Bearing at $3x10^6$DN," J. Lubr. Technol., 98(4), 580-585.

Barus, C. (1893) "Isotherms, Isopiestics, and Isometrics Relative to Viscosity," Am. J. Sci., 45, 87-96.

Barwell, F. T. (1974) "The Tribology of Wheel on Rail," Tribol. Int., 7, (4), 146-150.

Barwell, F. T. (1979) "Bearing Systems - Principles and Practice," Oxford University Press, Oxford.

Bell, J. C. and Kannel, J. W. (1970) "Simulation of Ball-Bearing Lubrication with a Rolling-Disk Apparatus," J. Lubr. Technol., 92, 1-15.

Bell, J. C., Kannel, J. W., and Allen, C. M. (1964) "The Rheological Behaviour of the Lubricant in the Contact Zone of a Rolling Contact System," J. Basic Eng., 86(3), 423-432.

Bisson, E. E. and Anderson, W. J. (1964) "Advanced Bearing Technology," NASA SP-38.

Biswas, S. and Snidle, R. W. (1976) "Elastohydrodynamic Lubrication of Spherical Surfaces of Low Elastic Modulus," J. Lubr. Technol., 98(4), 524-529.

Blok, H. (1952) Discussion of paper by E. McEwen. Gear Lubrication Symposium. Part I. The Lubrication of Gears, J. Inst. Petrol., 38, 673.

Blok, H. (1965) "Inverse Problems in Hydrodynamic Lubrication and Design Directives for Lubricated Flexible Surfaces," Proceedings of International Symposium on Lubrication and Wear, D. Muster and B. Sternlicht, eds., McCutchan, Berkeley, 1-151.

Brewe, D. E., Coe, H. H., and Scibbe, H. W. (1969) "Cooling Studies with High-Speed Ball Bearings Operating in Cool Hydrogen Gas," Trans. ASLE, vol. 12, 66-76.

Brewe, D. E. and Hamrock, B. J. (1977) "Simplified Solution for Elliptical-Contact Deformation Between Two Elastic Solids," J. Lubr. Technol. 99(4), 485-487.

Brewe, D. E., Hamrock, B. J., and Taylor, C. M. (1979) "Effect of Geometry on Hydrodynamic Film Thickness," J. Lubr. Technol., 101(2), 231-239.

Brown, P. F. and Potts, J. R. (1977) "Evaluation of Powder Processed Turbine Engine Ball Bearings," PWA-FR-8481, Pratt & Whitney Aircraft Group, West Palm Beach, Fla. (AFAPL-TR-77-26.)

Cameron, A. (1954) "Surface Failure in Gears," J. Inst. Petrol., vol. 40, 191.

Cameron, A. (1966) The Principles of Lubrication, Wiley, New York.

Cameron, A. and Gohar, R. (1966) "Theoretical and Experimental Studies of the Oil Film in Lubricated Point Contact," Proc. R. Soc. London, Ser. A., 291, 520-536.

Carburi, M. (1777) "Monument Elevé a la Gloire de Pierre-le-Grand, ou Relation Des Travaux et des Moyens Mechaniques Qui ont été employés pour transporter à Petersbourg un Rocher de trois millions pesant, destiné à servir de base à la Statue équestre de cet Empereur; avec un Examen Physique et Chymique de meme Rocher," Paris, (Bookseller: Nyon âiné, Libraine, rue Saint-Lean-de-Beauvois; Printer: Imprimeur-Libraire, rue de la Harpe, vis-à-vis la rue S. Severin).

Castle, P. and Dowson, D. (1972) "A Theoretical Analysis of the Starved Contact," Proceedings of Second Symposium on Elastohydrodynamic Lubrication, Institution of Mechanical Engineers, London, 131.

Cheng, H. S. (1967) "Calculation of Elastohydrodynamic Film Thickness in High-Speed Rolling and Sliding Contacts," Mechanical Technology Technical Report MTI-67TR24, May 1967.

Cheng, H. S. (1970) "A Numerical Solution to the Elastohydrodynamic Film Thickness in an Elliptical Contact," J. Lubr. Technol., 92(1), 155-162.

Cheng, H. S. and Orcutt, F. K. (1965-66) "A Correlation Between the Theoretical and Experimental Results on the Elastohydrodynamic Lubrication of Rolling and Sliding Contacts," Elastrohydrodynamic Lubrication, Symposium, Leeds, England, Sept. 21-23, 1965, General Papers. Institution of Mechanical Engineers, London, 111-121.

Cheng, H. S. and Sternlicht, B. (1964) "A Numerical Solution for the Pressure, Temperature, and Film Thickness Between Two Infinitely Long, Lubricated Rolling and Sliding Cylinders, Under Heavy Loads," J. Basic Eng. 87(3), 695-707.

Chiu, Y. P. (1974) "An Analysis and Prediction of Lubricant Film Starvation in Rolling Contact Systems," ASME Trans., 17(1), 22-35.

Clark, R. H. (1938) "Earliest Known Ball Thrust Bearing Used in Windmill," English Mechanic, 30 (Dec.) 223.

Coulomb, C. A. (1785) "Théorie des Machines Simples, en ayant égard au frottement de leur parties, et a la roideur des cordages," Academic Royale des Sciences, Mem. Math. Phys., X, Paris, 161-342.

Crook, A. W. (1957) "Simulated Gear-Tooth Contact: Some Experiments Upon Their Lubrication and Sub-Surface Deformation," Proc. Inst. Mech. Eng., London, 171, 187.

Crook, A. W. (1958) "The Lubrication of Rollers, I," Phil. Trans. R. Soc. London, Ser. A, 250, 387-409.

Crook, A. W. (1961) "Elasto-Hydrodynamic Lubrication of Rollers, Nature," 190, 1182.

Crook, A. W. (1963) "The Lubrication of Rollers, IV - Measurements of Friction and Effective Viscosity," Phil. Trans. R. Soc. London, Ser. A, 255, 281-312.

Dalmaz, G. and Godet, M. (1973) "Traction, Load, and Film Thickness in Lightly Loaded Lubricated Point Contacts," J. Mech. Eng. Sci., 15(6), 400-409.

Dalmaz, G. and Godet, M. (1978) "Film Thickness and Effective Viscosity of Some Fire Resistant Fluids in Sliding Point Contacts," J. Lubr. Technol., 100(2), 304-308.

Denhard, W. G. (1966) "Cost Versus Value of Ball Bearings," Gyro-Spin Axis Hydrodynamic Bearing Symposium, Vol. II, Ball Bearings. Massachusetts Institute of Technology, Cambridge, Mass., Tab. 1.

Desaguliers, J. T. (1734) A Course of Experimental Philosophy, 2 Volumes, London, Volume I, with 32 copper plates.

Dowson, D. (1962) "A Generalized Reynolds Equation for Fluid-Film Lubrication," Int. J. Mech. Sci., 4, 159-170.

Dowson, D. (1965) "Elastohydrodynamic Lubrication - An Introduction and a Review of Theoretical Studies," Institute of Mechanical Engineers, London, Paper R1, 7-15.

Dowson, D. (1968) "Elastohydrodynamics," Proc. Inst. Mech. Eng., London, 182(3A), 151-167.

Dowson, D. (1975) "The Inlet Boundary Condition," Cavitation and Related Phenomena in Lubrication. D. Dowson, M. Godet, and C. M. Taylor, eds., Mechanical Engineering Publications, Ltd., New York, 143-152.

Dowson, D. (1976) "The Origins of Rolling Contact Bearings," T. Sakuri, ed., Proceedings of JSLE-ASLE International Lubrication Conference, Elsevier, Amsterdam, 20-38.

Dowson, D. (1979) History of Tribology, Longman, London and New York.

Dowson, D. (1981) "Lubrication of Joints," Chapter 13 in "The Biomechanics of Joints and Joint Replacements," Edited by D. Dowson and V. Wright, Mechanical Engineering Publications, Bury St. Edmunds, Suffolk. (To be published.)

Dowson, D. and Hamrock, B. J. (1976) "Numerical Evaluation of the Surface Deformation of Elastic Solids Subjected to a Hertzian Contact Stress," ASLE Trans., 19(4), 279-286.

Dowson, D. and Higginson, G. R. (1959) "A Numerical Solution to the Elastohydrodynamic Problem," J. Mech. Eng. Sci., 1(1), 7-15.

Dowson, D. and Higginson, G. R. (1961) "New Roller-Bearing Lubrication Formula," Engineering London, vol. 192, 158.

Dowson, D. and Higginson, G. R. (1964), "A Theory of Involute Gear Lubrication," Institute of Petroleum Gear Lubrication; Proceedings of a Symposium organized by the Mechanical Tests of Lubricants Panel of the Institute, (1964), Elsevier, 8-15.

Dowson, D. and Higginson, G. R. (1966) Elastohydrodynamic Lubrication, The Fundamentals of Roller and Gear Lubrication. Pergamon, Oxford.

Dowson, D., Saman, W. Y., and Toyoda, S. (1979) "A Study of Starved Elastohydrodynamic Line Contacts," Proceedings of Fifth Leeds-Lyon Symposium on Tribology on 'Elastohydrodynamics and Related Topics,' D. Dowson, C. M. Taylor, M. Godet, and D. Berthe, eds., Mechanical Engineering Publications, Ltd., 92-103.

Dowson, D. and Swales, P. D. (1969) "The Development of Elastohydrodynamic Conditions in a Reciprocating Seal," Proceedings of Fourth International Conference on Fluid Sealing, Vol. 2, Paper 1, British Hydromechanics Research Association, 1-9.

Dowson, D. and Toyoda, S. (1979) "A Central Film Thickness Formula for Elastodydrodynamic Line Contacts." Proceedings of Fifth Leeds-Lyon Symposium on Tribology on 'Elastohydrodynamics and Related Topics,' D. Dowson, C. M. Taylor, M. Godet, and D. Berthe, eds., Mechanical Engineering Publications, Ltd., 104-115.

Dowson, D. and Whitaker, A. V. (1965-66) "A Numerical Procedure for the Solution of the Elastohydrodynamic Problems of Rolling and Sliding Contacts Lubricated by a Newtonian Fluid," Proc. Inst. Mech. Eng., London, 180(3B), 57.

Dyson, A. (1970) "Flow Properties of Mineral Oils in Elastohydrodynamic Lubrication," Phil. Trans. R. Soc. London, Ser. A, 258(1093), 529-564.

Dyson, A., Naylor, H., and Wilson, A. R. (1965-66) "The Measurement of Oil-Film Thickness in Elastohydrodynamic Contacts," Proceedings of Symposium on Elastohydrodynamic Lubrication, Leeds, England, Institution of Mechanical Engineers, London, 76-91.

Dupuit, A. J. E. J. (1839), "Résumé de Mémoire sur le tirage des voitures et sur le frottement de seconde espece," Competes rendus de l'Académie des Sciences, Paris, IX, 689-700, 775.

Eaton, J. T. H., ed. (1969) "A Trip Down Memory Lane," The Dragon, XLIV (5), 5-7.

ESDU (1965) "General Guide to the Choice of Journal Bearing Type," Engineering Sciences Data Unit, Item 65007, Institute of Mechanical Engineers, London.

ESDU (1967) "General Guide to the Choice of Thrust Bearing Type," Engineering Sciences Data Unit, Item 67033, Institution of Mechanical Engineers, London.

ESDU (1978) "Grease Life Estimation in Rolling Bearings," Engineering Sciences Data Unit, Item 78032, Institution of Mechanical Engineers, London.

ESDU (1978) "Contact Phenomena. I: Stresses, Deflections and Contact Dimensions for Normally-Loaded Unlubricated Elastic Components," Engineering Sciences Data Unit, Item 78035, Institution of Mechanical Engineers, London.

Evans, H. P., Biswas, S., and Snidle, R. W. (1978) "Numerical Solution of Isothermal Point Contact Elastohydrodynamic Lubrication Problems," Proceeding of First International Conference on Numerical Methods in Laminar and Turbulent Flow, Pentech Press, London, 639-656.

Evans, H. P. and Snidle, R. W. (1978) "Toward a Refined Solution of the Isothermal Point Contact EHD Problem." International Conference Fundmentals of Tribology, Massachusetts Institute of Technology, Cambridge, Mass., June 19-22, 1978.

Fein, R. S. (1968) Discussion on the Papers of J. K. Appeldorn and A. B. Metzner, J. Lubr. Technol., 90, 540-542.

Fellows, T. G., Dowson, D., Perry, F. G., and Plint, M. A. (1963) "Perbury Continuously Variable Ratio Transmission," in N. A. Carter, Ed. Advances in Automobile Engineering, Part 2; Pergamon Press, 123-139.

Foord, C. A., Hammann, W. C., and Cameron, A. (1968) "Evaluation of Lubricants Using Optical Elastohydrodynamics," ASLE Trans., 11, 31-43.

Foord, C. A., Wedeven, L. D., Westlake, F. J. and Cameron, A. (1969-70) "Optical Elastohydrodynamics," Proc. Inst. Mech. Eng., London, Part I, 184, 487-503.

Fromm, H. (1948), "Laminre Strömung Newtonscher und Maxwellscher Slüssigkeiten," Angew Math. Mech., 28(2), 43-54.

Furey, M. J. (1961) "Metallic Contact and Friction Between Sliding Surfaces," ASLE Trans., vol. 4, 1-11.

Gentle, C. R. and Cameron, A. (1973) "Optical Elastohydrodynamics at Extreme Pressure," Nature, 246(5434), 478-479.

Gohar, R. and Cameron A. (1966) "The Mapping of Elastohydrodynamic Contacts," ASLE Trans., 10, 215-225.

Goodman, J. (1912) "(1) Roller and Ball Bearings;" "(2) The Testing of Antifriction Bearing Materials," Proceedings of the Institute of Civil Engineers, CLXXXIX, Session 1911-12, Pt. III, pp. 4-88.

Greenwood, J. A. (1969) "Presentation of Elastohydrodynamic Film-Thickness Results." J. Mech. Eng. Sci., 11(2), 128-132.

Greenwood, J. A. and Kauzlarich, J. J. (1973) "Inlet Shear Heating in Elastohydrodynamic Lubrication," J. Lubr. Technol., 95(4), 401-416.

Grubin, A. N. (1949) "Fundamentals of the Hydrodynamic Theory of Lubrication of Heavily Loaded Cylindrical Surfaces," Investigation of the Contact Machine Components. Kh. F. Ketova, ed., Translation of Russian Book No. 30, Central Scientific Institute for Technology and Mechanical Engineering, Moscow, Chapter 2. (Available from Dept. of Scientific and Industrial Research, Great Britain, Transl. CTS-235, and from Special Libraries Association, Chicago, Trans. R-3554.)

Gunther, R. T. (1930), Early Science in Oxford, Volumes VI and VII, "The Life and Work of Robert Hooke," Vol. VII, Pt. II, 666-679, printed for the author at the Oxford University Press by John Johnson (Oxford).

Hall, L. F. (1957) "A Review of the Papers on the Lubrication of Rotating Bearings and Gears," Proceedings of Conference on Lubrication and Wear, Institution of Mechanical Engineers, pp. 425-429.

Hamilton, G. M. and Moore, S. L. (1971) "Deformation and Pressure in an Elastohydrodynamic Contact," Proc. R. Soc., London, Ser. A, 322, 313-330.

Halling, J. (1976) Introduction of Tribology, Wykeham Publ., London.

Hamrock, B. J. (1976) Elastohydrodynamic Lubrication of Point Contacts, Ph.D. Dissertation, University of Leeds, Leeds, England.

Hamrock, B. J. and Anderson, W. J. (1973) "Analysis of an Arched Outer-Race Ball Bearing Considering Centrifugal Forces," J. Lubr. Technol., 95(3), 265-276.

Hamrock, B. J. and Dowson, D. (1974) "Numerical Evaluation of Surface Deformation of Elastic Solids Subjected to Hertzian Contact Stress," NASA TN D-7774.

Hamrock, B. J. and Dowson, D. (1976a) "Isothermal Elastohydrodynamic Lubrication of Point Contacts, Part I - Theoretical Formulation," J. Lubr. Technol., 98(2), 223-229.

Hamrock, B. J. and Dowson, D. (1976b) "Isothermal Elastohydrodynamic Lubrication of Point Contacts, Part II - Ellipticity Parameter Results," J. Lubr. Technol., 98(3), 375-378.

Hamrock, B. J. and Dowson, D. (1977a) "Isothermal Elastohydrodynamic Lubrication of Point Contacts, Part III - Fully Flooded Results," J. Lubr. Technol., 99(2), 264-276.

Hamrock, B. J. and Dowson, D. (1977b) "Isothermal Elastohydrodynamic Lubrication of Point Contacts, Part IV - Starvation Results," J. Lubr. Technol., 99(1), 15-23.

Hamrock, B. J. and Dowson, D. (1978) "Elastohydrodynamic Lubrication of Elliptical Contacts for Materials of Low Elastic Modulus, Part I - Fully Flooded Conjunction," J. Lubr. Technol., 100(2), 236-245.

Hamrock, B. J. and Dowson, D. (1979a) "Elastohydrodynamic Lubrication of Elliptical Contacts for Materials of Low Elastic Modulus, Part II - Starved Conjunction," J. Lubr. Technol., 101(1), 92-98.

Hamrock, B. J. and Dowson, D. (1979b) "Minimum Film Thickness in Elliptical Contacts for Different Regimes of Fluid-Film Lubrication," Proceedings of Fifth Leeds-Lyon Symposium on Tribology on 'Elastohydrodynamics and Related Topics,' D. Dowson, C. M. Taylor, M. Godet, and D. Berthe, eds., Mechnical Engineering Publications, Ltd., 22-27.

Hardy, W. B. and Doubleday, I. (1922a) "Boundary Lubrication - the Temperature Coefficient," Proc. R. Soc. London, Ser. A, 101, 487-492.

Hardy, W. B. and Doubleday, I. (1922b) "Boundary Lubrication - the Paraffin Series," Proc. R. Soc. London, Ser. A., 100, 550-574.

Harris, T. A. (1966) Rolling Bearing Analysis. Wiley, New York.

Harris, T. A. (1971) "An Analytical Method to Predict Skidding in Thrust-Loaded, Angular-Contact Ball Bearings," J. Lubr. Technol., vol. 93, 17-24.

Harrison, H. C. (1949) The Story of Sprowston Mill, Phoenix House, London.

Harrison, W. J. (1913) "The Hydrodynamical Theory of Lubrication with Special Reference to Air as a Lubricant," Trans. Cambridge Philos. Soc., xxii (1912-25), 6-54.

Harrison, G. and Trachman, E. G. (1972) "The Role of Compressional Viscoelasticity in the Lubrication of Rolling Contacts," J. Lubr. Technol., 94, 306-312.

Heathcote, H. L. (1921) "The Ball Bearing: In the Making, Under Test, and on Service," Proc. Instn. Automotive Engrs., London, 15, pp. 569-702.

Herrebrugh, K. (1968) "Solving the Incompressible and Isothermal Problem in Elastohydrodynamic Lubrication Through an Integral Equation," J. Lubr. Technol., 90(1), 262-270.

Hersey, M. D. (1966) Theory and Research in Lubrication - Foundations for Future Developments, Wiley, New York.

Hersey, M. S. and Hopkins, R. F. (1954) "Viscosity of Lubricants Under Pressure. Coordinated Data from Twelve Investigations." ASME, New York.

Hertz, H. (1881) "The Contact of Elastic Solids," J. Reine Angew. Math., 92, 156-171.

Hooke, C. J. (1977) "The Elastohydrodynamic Lubrication of Heavily Loaded Contacts," J. Mech. Eng. Sci., 19(4), 149-156.

Hirst, W. and Moore, A. J. (1974) "Non-Newtonian Behavior in Elastohydrodynamic Lubrication," Proc. R. Soc. London, Ser. A, 337, 101-121.

Houghton, P. S. (1976) Ball and Roller Bearings, Applied Science Publishers, Ltd., London.

Jacobson, B. (1970) "On the Lubrication of Heavily Loaded Spherical Surfaces Considering Surface Deformations and Solidification of the Lubricant." Acta Polytech. Scand., Mech. Eng. Ser. No. 54.

Jacobson, B. (1972) "Elasto-Solidifying Lubrication of Spherical Surfaces." American Society of Mechanical Engineers Paper No. 72-LUB-7.

Jacobson, B. (1973) "On the Lubrication of Heavily Loaded Cylindrical Surfaces Considering Surface Deformations and Solidification of the Lubricant," J. Lubr. Technol., 95(3), 321-27.

Jamison, W. E., Lee, C. C., and Kauzlarich, J. J. (1978) "Elasticity Effects on the Lubrication of Point Contacts," ASLE Trans., 21(4), 299-306.

Johnson, B. L. (1964) "A 'Stainless High Speed' Steel for Aerospace Applications," Metal Prog., 86(3), 116-118.

Johnson, B. L. (1965) "High Temperature Wear Resisting Steel," U.S. Patent No. 3,167,423, Jan. 1965.

Johnson, K. L. (1970) "Regimes of Elastohydrodynamic Lubrication." J. Mech. Eng. Sci., 12(1), 9-16.

Johnson, K. L. and Cameron, R. (1967) "Shear Behavior of Elastohydrodynamic Oil Films at High Rolling Contact Pressures," Proc. Ins. Mech. Eng., Part 1, 182, 307-319.

Johnson, K. L. and Roberts, A. D. (1974) "Observation of Viscoelastic Behaviour of an Elastohydrodynamic Lubricant Film," Proc. R. Soc. London, Ser. A, 337, 217-242.

Johnson, K. L. and Tevaarwerk, J. L. (1977) "Shear Behaviour of Elastohydrodynamic Oil Films," Proc. R. Soc. London, Ser. A, 356, 215-236.

Jones, A. B. (1946) "Analysis of Stresses and Deflections," New Departure Engineering Data, General Motors Corp., Bristol, Conn.

Jones, A. B. (1956) "The Mathematical Theory of Rolling-Element Bearings," Mechanical Design and Systems Handbook.

Kannel, J. W., Bell, J. C., and Allen, C. M. (1964) "Methods for Determining Pressure Distribution in Lubricated Rolling Contact," ASLE Paper 64-LC-23, Presented at ASME-ASLE Lubrication Conference, Washington, D.C., Oct. 13-16, 1964.

Kakuta, K. (1979) "The State of the Art of Rolling Bearings in Japan," Bull. Japan Soc. Prec. Eng., 13(4), 169-176.

Kapitza, P. L. (1955) "Hydrodynamic Theory of Lubrication During Rolling," Zh. Tekh. Fiz., 25(4), 747-762.

Koye, K. A. and Winer, W. O. (1980) " An Experimental Evaluation of the Hamrock and Dowson Minimum Film Thickness Equation for Fully Flooded EHD Point Contacts," International ASME/ASLE Lubrication Conference, San Francisco, August 1980.

Kunz, R. K. and Winer, W. O. (1977) Discussion 275-276, to Hamrock, B. J. and Dowson, D. "Isothermal Elastohydrodynamic Lubrication of Point Contacts, Part III - Fully Flooded Results," J. Lubr. Technol., 99(2), 264-275.

Lane, T. B. (1951) "Scuffing Temperatures of Boundary Lubricant Films," Br. J. Appl. Phys., 2, (Suppl. 1), 35-38.

Lane, T. B. and Hughes, J. R. (1952) "A Study of the Oil Film Formation in Gears by Electrical Resistance Measurements," Br. J. Appl. Phys., 3(10), 315-318.

Lamb, H. (1932) Hydrodynamics. Cambridge University Press.

Layard, A. H. (1849) Nineveh and Its Remains, Vols. I and II, John Murray, London.

Layard, A. H. (1853) Discoveries in the Ruins of Nineveh and Babylon, Vols. I and II, John Murray, London.

Lee, D., Sanborn, D. M., and Winer, W. O. (1973) "Some Observations of the Relationship Between Film Thickness and Load in High Hertz Pressure Sliding Elastohydrodynamic Contacts," J. Lubr. Technol., 95(3), 386.

Leibnitz, G. W. (1706) "Tentamen de natura et remedlie resistenziarum in machines," Miscellanea Berolinensia. Class. mathem, 1710, (Jean Boudot, Paris), 1, 307.

Lewicki, W. (1955) "Some Physical Aspects of Lubrication in Rolling Bearings and Gears," Engineer, 200 (5193), 176-178, and (5194), 212-215.

Lundberg, G. and Palmgren, A. (1947) "Dynamic Capacity of Rolling Bearings," Acta Polytech., Mech. Eng. Sci., 1(3).

Martin, H. M. (1916) "Lubrication of Gear Teeth," Engineering, London, 102, 199.

McEwen, E. (1952) "The Effect of Variation of Viscosity with Pressure on the Load Carrying Capacity of Oil Films Between Gear Teeth," J. Inst. Petrol., 38, 646.

Meldahl, A. (1941) "Contribution to the Theory of the Lubrication of Gears and of the Stressing of the Lubricated Flanks of Gear Teeth," Brown Boveri Review, 28(11), 374.

Merritt, H. E. (1935) "Worm-Gear Performance," Proc. Inst. Mech. Eng., London, 129, 127-158.

Meyer, D. R. and Wilson, C. C. (1971) "Measurement of Elastohydrodynamic Oil Film Thickness and Wear in Ball Bearings by the Strain Gage Method," J. Lubr. Technol., 93(2), 224-230.

Moes, H. (1965-66) "Communication, Elastohydrodynamic Lubrication," Proc. Inst. Mech. Eng., London, 180(3B), 244-245.

Moes, H. and Bosma, R. (1972) "Film Thickness and Traction in EHL at Point Contact," Proceedings of Second Symposium on Elastohydrodymamic Lubrication, Leeds, England, Institution of Mechanical Engineers, London, 149.

Moore, A. J. (1973) "Non-Newtonian Behaviour in Elastohydrodynamic Lubrication," Ph.D. Thesis, University of Reading.

Morgan, M. H. and Warren, H. L. (1960) Translation of Vitruvius: The Ten Books of Architecture, Dover, New York.

Morin, A. J. (1835) "Nouvelles expériences faites à Metz en 1833 sur le frottement, sur la transmission due movement par le choc, sur le résistance des milieun imparfaits a le pénétration des projectiles, et sur le frottement pendant le choc," Mem. Savans Etrang. (Paris), VI, 641-785; Ann. Min. X, (1836), 27-56.

Nagaraj, H. S., Sanborn, D. M., and Winer, W. O. (1977) "Effects of Load, Speed, and Surface Roughness on Sliding EHD Contact Temperature," J. Lubr. Technol., 99(4), 254-263.

Navier, C. L. M. H. (1823) "Memoire sur les lois du mouvement des fluides," Mem. Acad. R. Sci., 6(2), 389-440.

Needham, J. (1965) Science and Civilization in China, Vol. 4, Physics and Physical Technology, Part II, Mechanical Engieering, Cambridge University Press.

Newton, I. (1687) Philosophiae Naturales Principia Mathematica, Imprimature S. Pepys, Reg. Soc. Praeses, 5 Julii 1686. Revised and supplied with a historical and explanatory appendix by F. Cajori, edited by R. T. Crawford (1934), and published by the University of California Press, Berkeley and Los Angeles (1966).

Orcutt, F. K. and Cheng, H. S. (1966) "Lubrication of Rolling-Contact Instrument Bearings," Gyro-Spin Axis Hydrodynamic Bearing Symposium, Vol. 2, Ball Bearings, Massachusetts Institute of Technology, Cambridge, Mass., Tab. 5.

Pai, S. I (1956) Viscous Flow Theory, Vol. I - Laminar Flow. Van Nostrand Reinhold, New Jersey.

Palmgren, A. (1945) "Ball and Roiller Bearing Engineering," S. K. F. Industries, Philadelphia.

Parker, R. J. and Hodder, R. S. (1978) "Roller-Element Fatigue Life of AMS 5749 Corrosion Resistant, High Temperature Bearing Steel," J. Lubr. Technol., 100(2), 226-235.

Parker, R. J. and Kannel, J. W. (1971) "Elastohydrodynamic Film Thickness Between Rolling Disks with a Synthetic Paraffinic Oil to 589 K (600° F); NASA TN D-6411.

Parker, R. J. and Zaretsky, E. V. (1978) "Rolling-Element Fatigue Life of AISI M-50 and 18-4-1 Balls." NASA TP-1202.

Peppler, W. (1936) "Untersuchunge uber die Drukubertragung bei Balasteten und Geschmierten um Laufenden Achsparallelen Zylinder," Maschinenelemente-Tagung Archen 1935, 42; V. D. I. Verlag, Berlin, 1936.

Peppler, W. (1938) "Druchubertragung an Geschmeirten Zylindriachen Gleit und Wälzflächen," V. D. I. Forschungshaft, 391.

Petrov, N. P. (1883) "Friction in Machines and the Effect of the Lubricant," Inzh. Zh., St. Peterb., 1, 71-140; 2, 227-279; 3, 377-436; 4, 535-564.

Petrusevich, A. S. (1951) "Fundamental Conclusion from the Contact-Hydrodynamic Theory of Lubrication," dzo. Akad. Nauk. SSSR (OTN), 2, 209.

Piggott, S. (1968) "The Earliest Wheeled Vehicles and the Caucasian Evidence," Proc. Prehist. Soc., XXXIV, (8), 266-318.

Pirvics, J. (1980) "Numerical Analysis Techniques and Design Methology for Rolling Element Bearing Load Support Systems," in International Conference on Bearing Design: Historical Aspects, Present Technology and Future Problems; Century 2 - Emerging Technology, W. J. Anderson, ed., American Society of Mechanical Engineers, New York, 1980, 47-85.

Plint, M. A. (1967) "Traction in Elastohydrodynamic Contact," Proc. Inst. Mech. Eng., London, Part 1, 182(14), 300-306.

Poritsky, H., Hewlett, C. W., Jr., and Coleman, R. E., Jr. (1947) "Sliding Friction of Ball Bearings of the Pivot Type," J. Appl. Mech., 14(4), 261-268.

Pritchard, C. (1981) "Traction Between Rolling Steel Surfaces - A Survey of Railway and Laboratory Services," Proceedings of the 7th Leeds-Lyon Symposium on 'Friction and Traction, Leeds, September 1980, Mechanical Engineering Publications. (To be published.)

Ramelli, A. (1588) "Le Diverse et Artificiose Machine," Paris, France.

Ranger, A. P., Ettles, C. M. M., and Cameron, A. (1975) "The Solution of Point Contact Elastohydrodynamic Problem," Proc. R. Soc. London, Ser. A, 346, 277-244.

Reti, L. (1971) "Leonardo on Bearings and Gears," Scientific American, 224, (2), 101-110.

Reynolds, O. (1875) "On Rolling Friction," Phil. Trans. R. Soc., 166, Pt. 1, 155.

Reynolds, O. (1886) "On the Theory of Lubrication and Its Application to Mr. Beauchamp Tower's Experiments, Including an Experimental Determination of the Viscosity of Olive Oil," Philos. Trans. R. Soc. London, 177, 157-234.

Roelands, C. J. A. (1966) Correlational Aspects of the Viscosity-Temperature-Pressure Relationship of Lubricating Oils. Druk. V. R. B., Groningen, Netherlands.

Rowe, J. (1734) "All Sorts of Wheel-Carriage Improved," printed for Alexander Lyon under Tom's Coffee House in Russell Street, Covent Garden, London.

Sanborn, D. M. (1969) "An Experimental Investigation of the Elastohydrodynamic Lubrication of Point Contacts in Pure Sliding," Ph.D. Thesis, University of Michigan.

Schlatter, R. (1974) "Double Vacuum Melting of High Performance Bearing Steels," Ind. Heat. 41(9), 40-55.

Shaw, M. C. and Macks, E. F. (1949) Analysis and Lubrication of Bearings, McGraw-Hill, New York.

Sibley, L. B., Bell, J. C., Orcutt, F. K., and Allen, C. M. (1960) "A Study of the Influence of Lubricant Properties on the Performance of Aircraft Gas Turbine Engine Rolling Contact Bearings," WADD Technical Report, 60-189.

Sibley, L. B. and Orcutt, F. K. (1961) "Elasto-Hydrodynamic Lubrication of Rolling Contact Surfaces," Trans. Amer. Soc. Lub. Engrs., 4(2), 234.

Smith, F. W. (1959) "Lubricant Behavior in Concentrated Contact Systems - The Caster Oil - Steel System," Wear, 2(4), 250-264.

Smith, F. W. (1962) The Effect of Temperature in Concentrated Contact Lubrication. ASLE Trans. 5(1), 142-148.

Stokes, G. G. (1845) "On the Theory of Internal Friction of Fluids in Motion," Trans. Cambridge Philos. Soc. 8, 287-319.

Stribeck, R. (1901) " Kugellager fur beliebige Belastungen," Z. Ver. dt. Ing., 45(3), 73-125.

Stribeck, R (1907) "Ball Bearings for Various Loads" - translation by H. Hess, Trans. Am. Soc. Mech. Engrs., 29, 420.

Swingler, C. L. (1980) "Surface Roughness in Elastohydrodynamic Line Contacts," Ph.D. Thesis, University of London (Imperial College).

Tabor, D. (1962) "Introductory Remarks," in Rolling Contact Phenomena, J. B. Bidwell, ed., Elsevier, Amsterdam, 1-5.

Tallian, T. E. (1969) "Progress in Rolling Contact Technology," Report AL 690007, SKF Industries, King of Prussia, Pa.

Tallian, T., Sibley, L., and Valori, R. (1965) "Elastohydrodynamic Film Effects on the Load-Life Behavior of Rolling Contacts," ASMS Paper 65-LubS-11.

Theyse, F. H. (1966) "Some Aspects of the Influence of Hydrodynamic Film Formation on the Contact Between Rolling/Sliding Surfaces," Wear, 9, 41-59.

Thorp, N. and Gohar, R. (1972) "Oil Film Thickness and Shape for a Ball Sliding in a Grooved Raceway," J. Lubr. Technol., 94(3), 199-210.

Timoshenko, S. and Goodier, J. N. (1951) Theory of Elasticity, 2nd ed., McGraw-Hill, New York.

Trachman, E. G. and Cheng, H. S. (1972) "Thermal and Non-Newtonian Effects on Traction in Elastohydrodynamic Contacts," Proceedings of Second Symposium on Elastohydrodynamic Lubrication, Institution of Mechanical Engineers, London, 142-148.

Tower, B. (1883) "First Report on Friction Experiments (Friction of Lubricated Bearings)," Proc. Inst. Mech. Eng., London, 632-659.

Turchina, V., Sanborn, D. M., and Winer, W. O. (1974) "Temperature Measurements in Sliding Elastohydrodynamic Point Contacts," J. Lubr. Technol., 96(3), 464-471.

Ucelli, G. (1940) "Le Navi Di Nemi," La Liberia Dello Stato, Roma.

Valori, R. (1978) Discussion to Parker, R. J. and Hodder, R. S. (1978) Rolling-Element Fatigue Life of AMS 5749 Corrosion Resistant, High Temperature Bearing Steel," J. Lubr. Technol., 100(2), 226-235.

Van Natrus, L., Polly, J., and Van Vuuren, C. (1734 and 1736), Groot Volkomen Moolenbock, 2 Volumes, Amsterdam.

Varlo, C. (1772) "Reflections Upon Friction with a Plan of the New Machine for Taking It Off in Wheel-Carriages, Windlasses of Ships, etc., Together with Metal Proper for the Machine, the Full Directions for Making It."

Vaughan, P. (1794) "Axle Trees, Arms, and Boxes," British Patent No. 2006 of A.D. 1794, 1-2, accompanied by 11 diagrams on one sheet.

Wailes, R. (1954) The English Windmill, Routledge & Kegan Paul, London.

Wailes, R. (1957) "Windmills" in History of Technology, C. Singer, E. J. Holmyard, A. R. Hall, and T. I. Williams, eds., Volume III, Oxford University Press, pp. 89-109.

Weber, C. and Saalfeld, K. (1954) Schmierfilm bei Walzen mit Verformung, Zeits ang. Math. Mech. 34 (Nos. 1-2).

Wedeven, L. E., Evans, D., and Cameron, A. (1971) "Optical Analysis of Ball Bearing Starvation," J. Lubr. Technol., 93(3), 349-363.

Weibull, W. (1949) "A Statistical Representation of Fatigue Failures in Solids," Trans. Roy. Inst. Technol., (27), Stockholm.

Whomes, T. L. (1966) The Effect of Surface Quality of Lubricating Film Performance, Ph.D. Dissertation, University of Leeds, Leeds, England.

Wilcock, D. F. and Booser, E. R. (1957) Bearing Design and Application. McGraw-Hill, New York.

Willis, T., Seth, B., and Dave, M. (1975) "Evaluation of a Diffraction Method for Thickness Measurement of Oil-Filled Gaps," J. Lubr. Technol. 97(4), 649-650.

Wilson, A. R. (1979) "The Relative Thickness of Grease and Oil Films in Rolling Bearings," Proc. Inst. Mech. Eng., London, 193(17), 185-192.

Winn, L. W., Eusepi, M. W., and Smalley, A. J. (1974) "Small, High-Speed Bearing Technology for Cryogenic Turbo-Pumps," MTI-74TR29, Mechanical Technology, Inc., Latham, N.Y. (NASA CR-134615.)

Wolveridge, P. E., Baglin, K. P., and Archard, J. G. (1971) "The Starved Lubrication of Cylinders in Line Contact," Proc. Inst. Mech. Eng., London, 185(1), 1159-1169.

Zaretsky, E. V., Anderson, W. J., and Bamberger, E. N. (1969) "Rolling Element Bearing Life for 400° to 600° F." NASA TN D-5002.

Zaretsky, E. V., Parker, R. J., and Anderson, W. J. (1967) "Component Hardness Differences and Their Effect on Bearing Fatigue," J. Lubr. Technol., 87(1), 47-62.

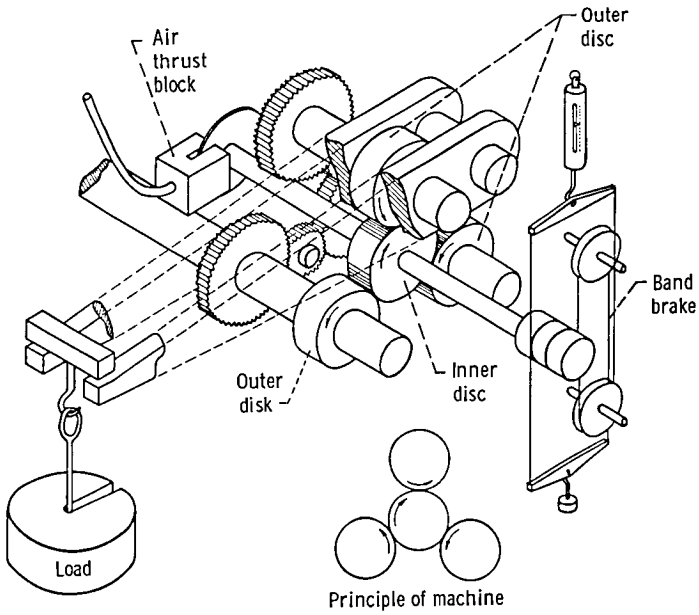

Figure 10.1. - Four-disc machine. (From Archard, 1965-66.)

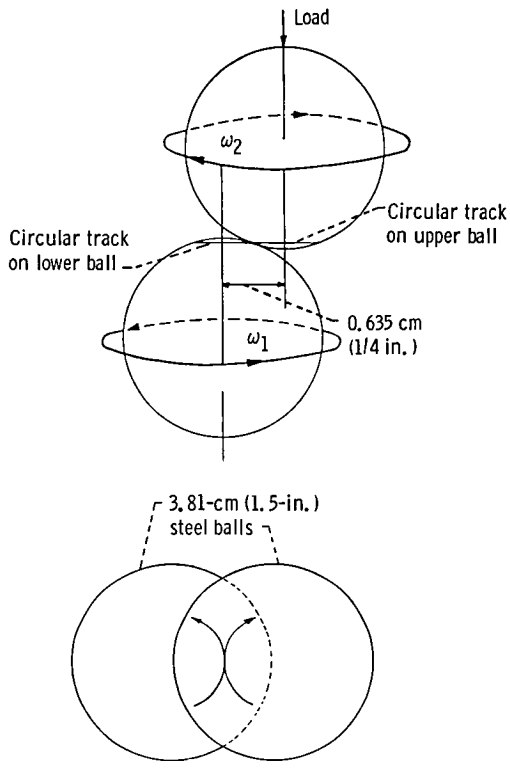

Figure 10.2. - Principle of two-ball machine. (From Archard, 1965-66.)

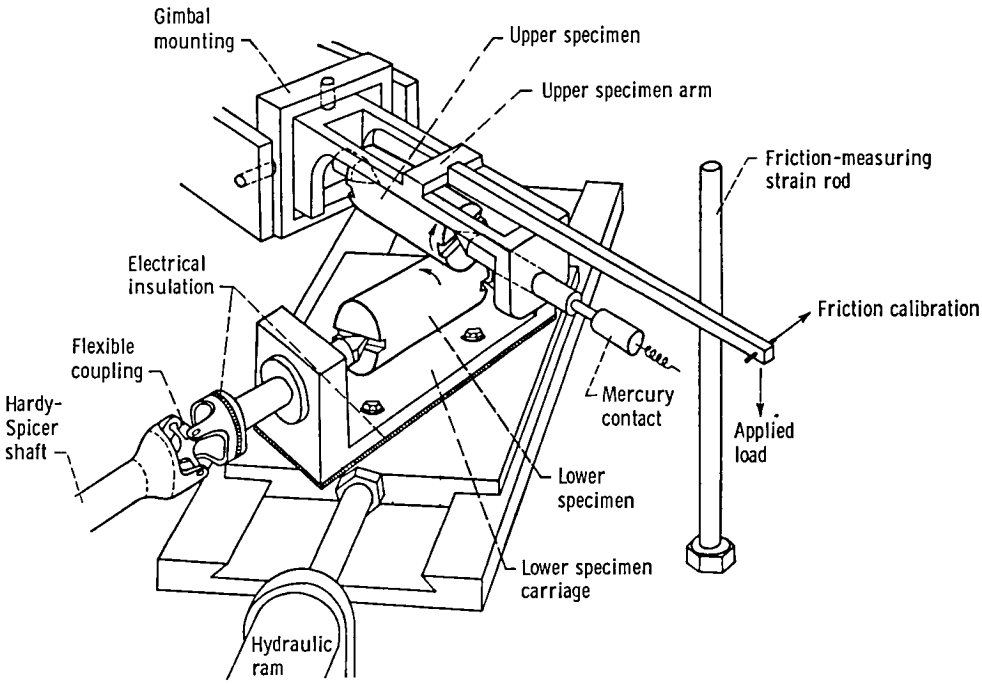

Figure 10.3. - Crossed-cylinders machine. (From Archard, 1965-66.)

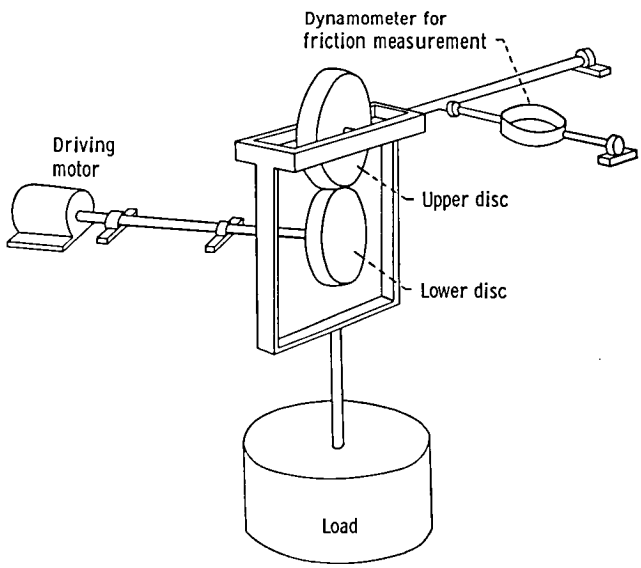

Figure 10.4. - Crossed-axes rolling disc machine. (From Archard, 1965-66.)

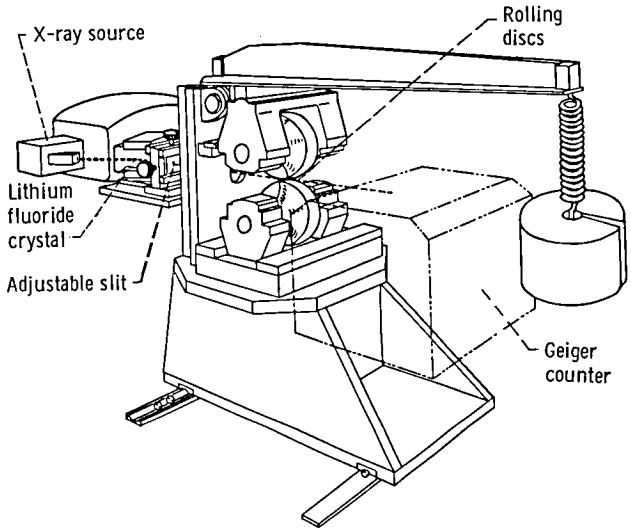

Figure 10.5.- Battelle precision disc machine and associated equipment for measuring film thickness with X-rays (motor drives omitted). (From Archard, 1965-66.)

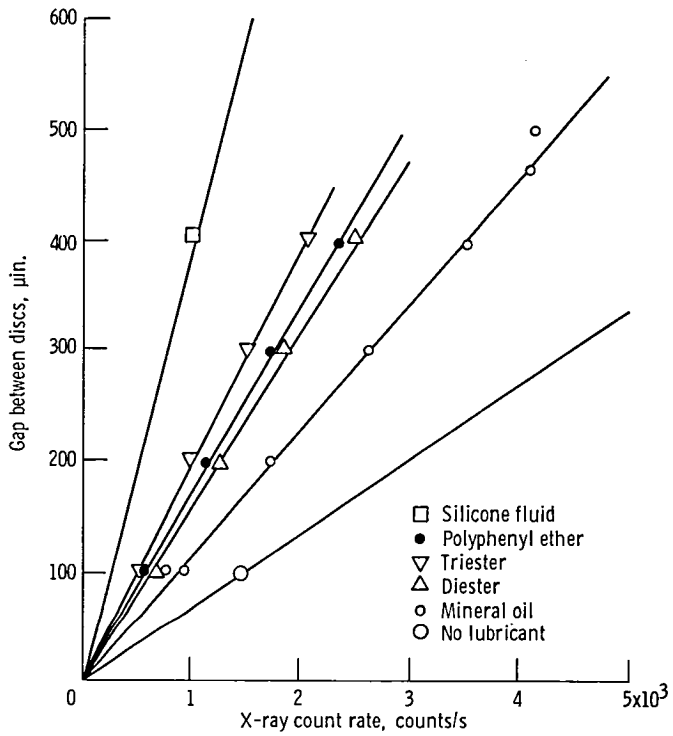

Figure 10.6. - Typical calibration curve for X-ray technique, obtained by using screw adjustment to separate discs. (From Bell and Kannel, 1970.)

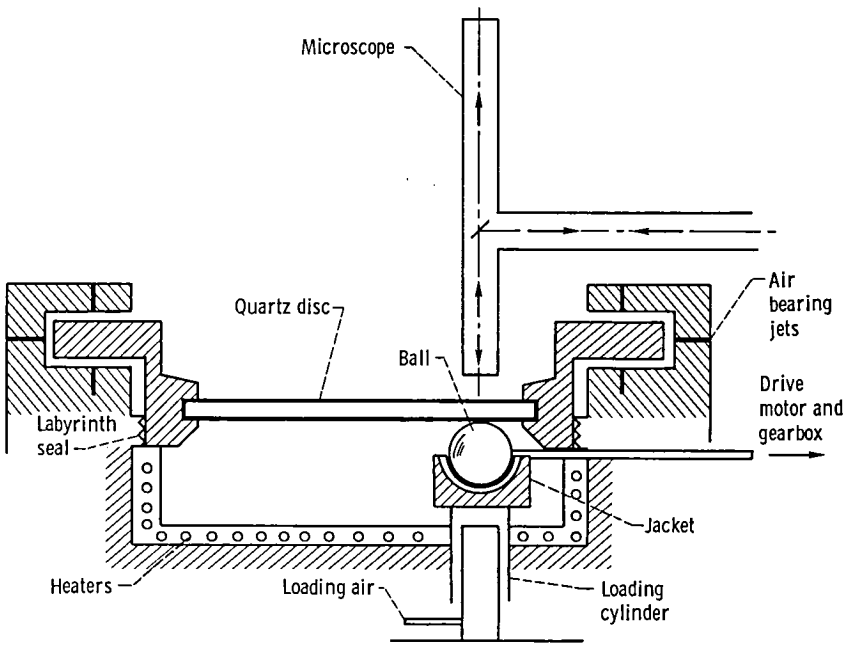

Figure 10.7. - Apparatus associated with interferometry technique. (From Foord, et al., 1969-70.)

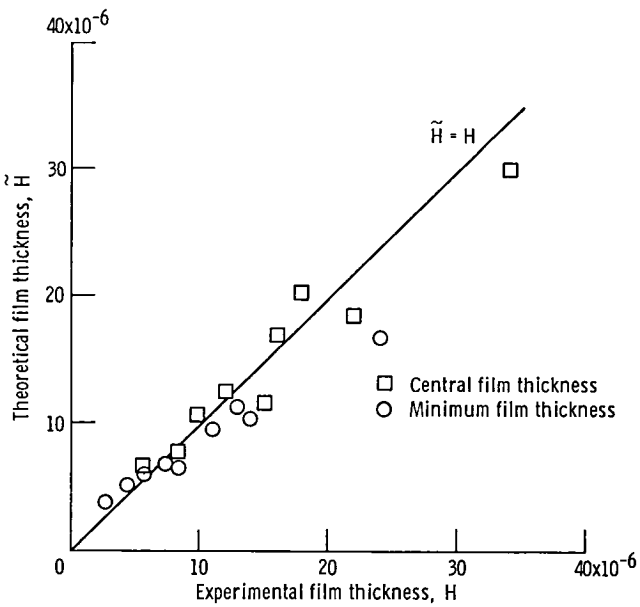

Figure 10.8. - Theoretical and experimental central and minimum film thicknesses based on optical interferometry studies by Kunz and Winer (1977). The dimensionless load parameter W is 0.1238×10^{-6}.

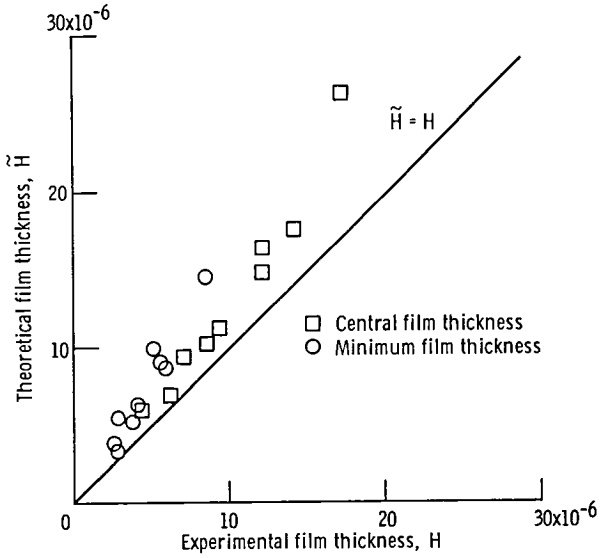

Figure 10.9.- Theoretical and experimental central and minimum film thicknesses for pure sliding. The dimensionless load parameter W is 0.928×10^{-6}. (From Kunz and Winer, 1977.)

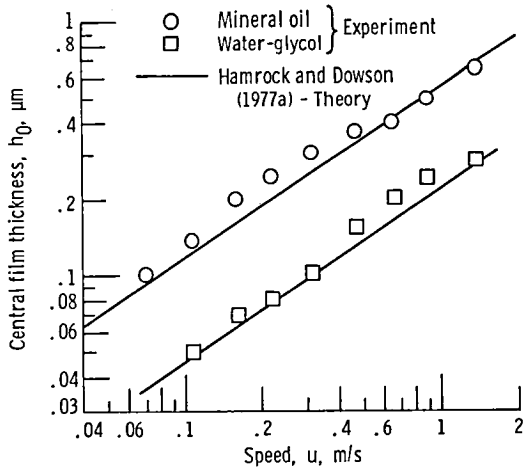

Figure 10.10.- Effect of speed on central film thickness at constant load (2.6 N) for mineral oil and water-glycol lubricants of similar viscosity. (From Dalmaz and Godet, 1978.)

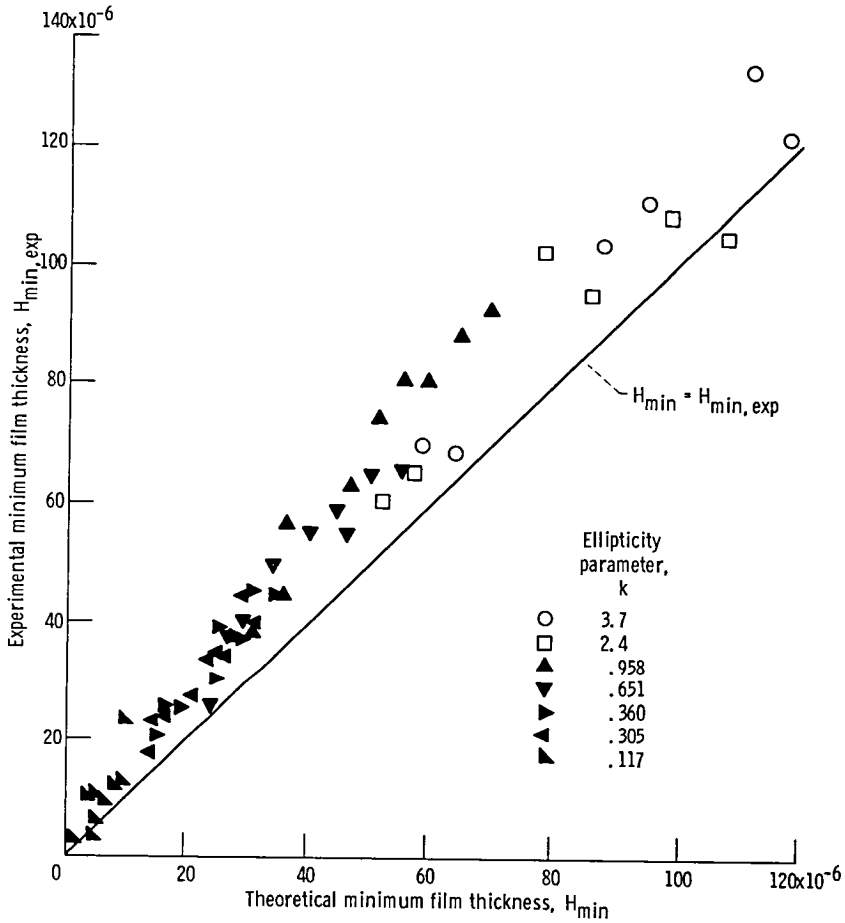

Figure 10.11. - Predicted dimensionless minimum film thickness from Hamrock and Dowson, equation (8.23), as function of measured dimensionless minimum film thickness.

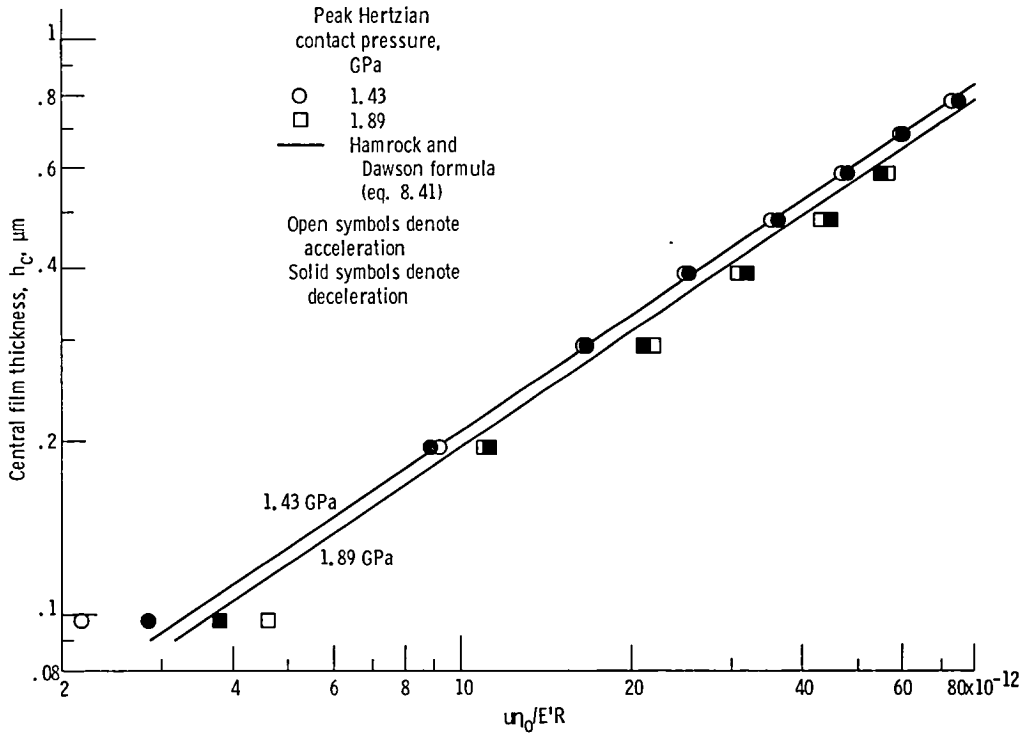

Figure 10.12. - Comparison between experiment and theoretical (eq. 8-41) values of central film thickness in pure rolling.

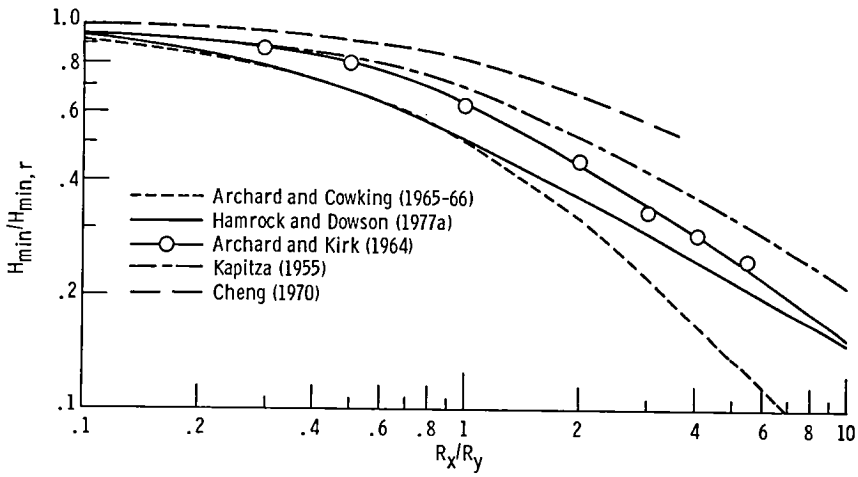

Figure 10.13. - Side-leakage factor for elliptical contacts.

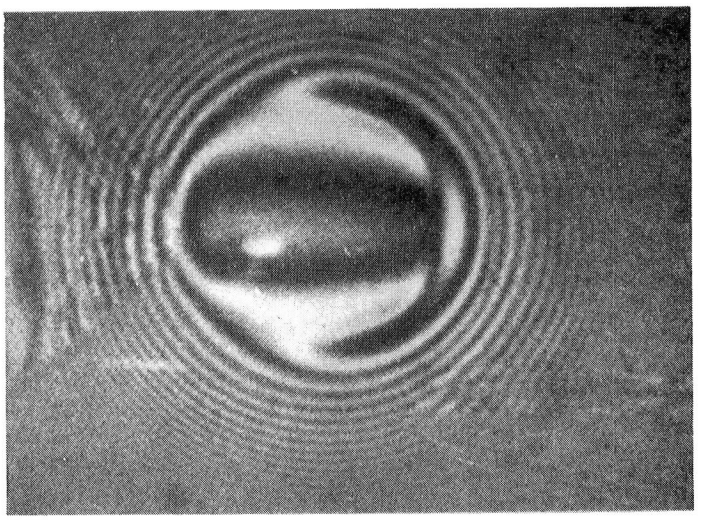

Figure 10.14. - Starved elastohydrodynamic conjunction. (From Sanborn, 1969.)

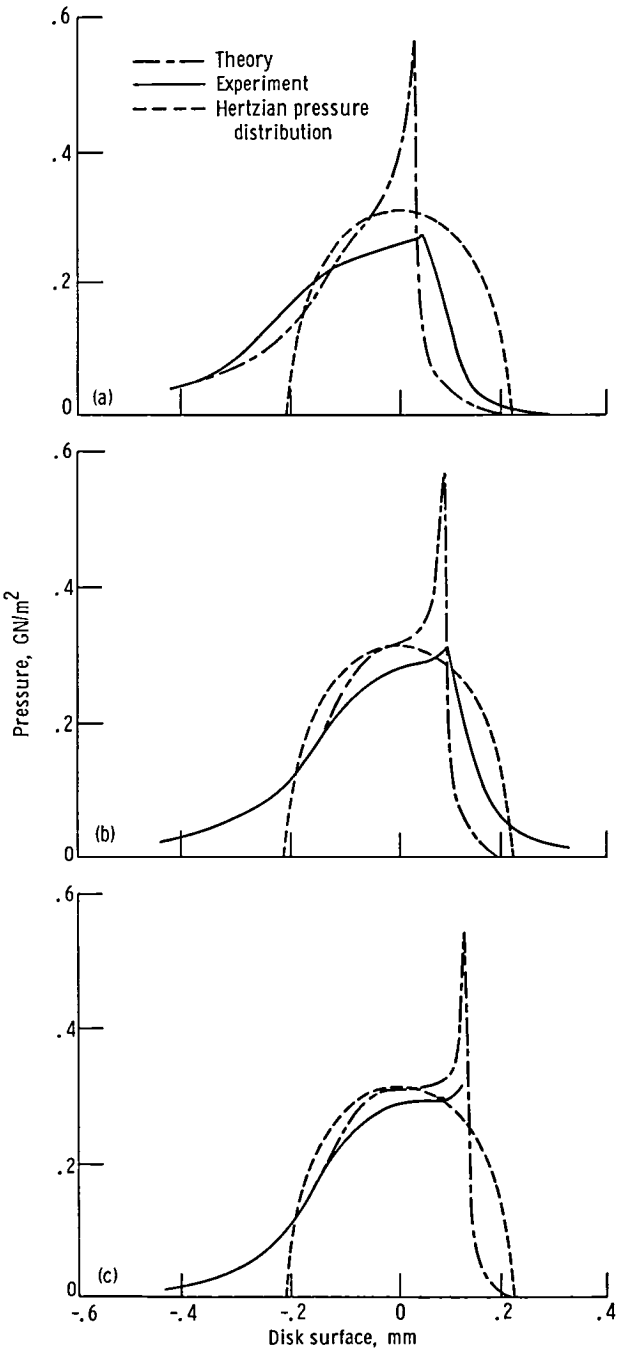

(a) u = 5.18 m/s.
(b) u = 26.9 m/s.
(c) u = 130 m/s.

Figure 10.15. - Calculated and experimental pressure distributions for a range of sliding speeds at constant load (100.3 kN/m).

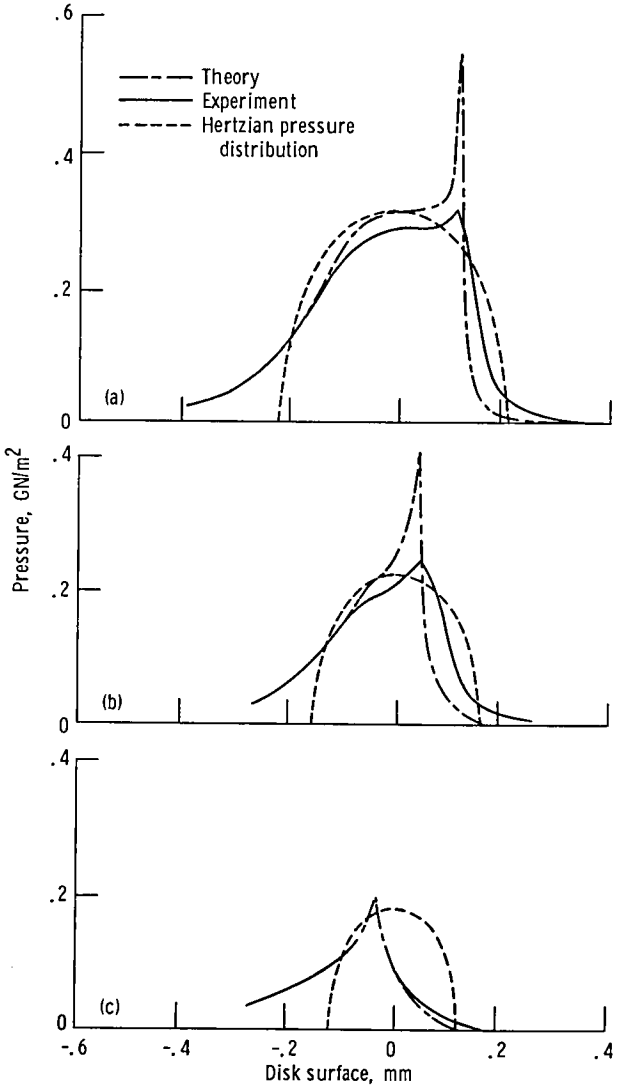

Figure 10.16. - Calculated and experimental pressure distributions for a range of loads at constant sliding speed (1.30 m/s).

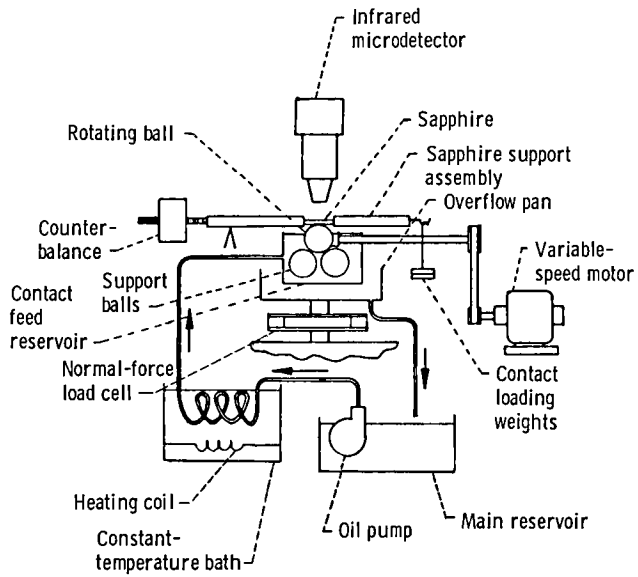

Figure 10.17. - Test apparatus used for temperature measurements. (From Nagaraj, et al., 1977.)

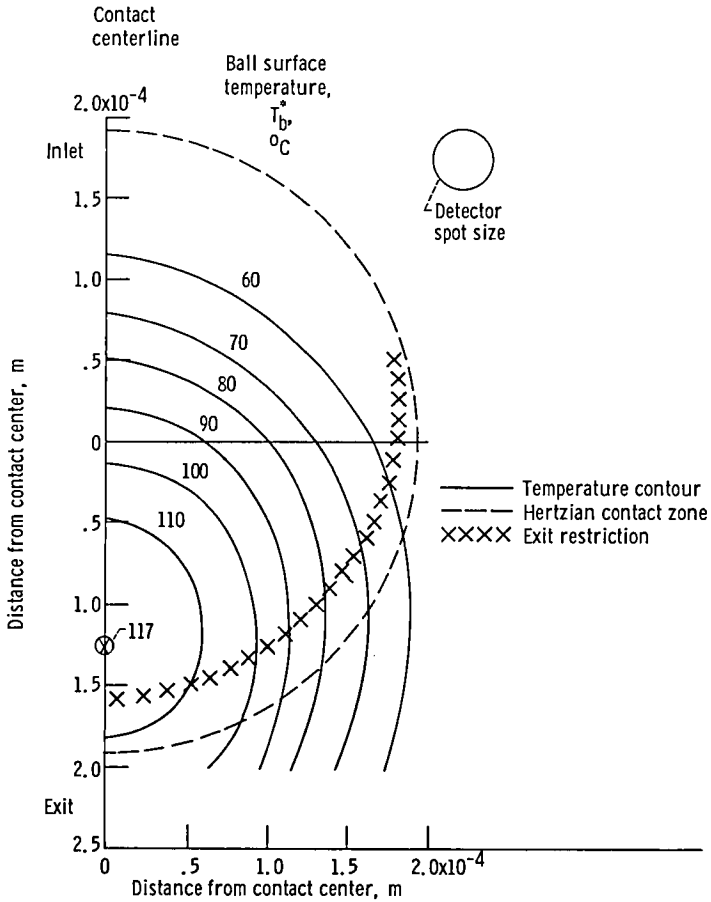

Figure 10.18. - Ball surface temperature. Sliding speed, u, 1.4 m/s; load, F, 67 N; maximum Hertzian pressure, P_{Hz}, 1.0 GN/m^2. (From Ausherman, et al., 1976.)

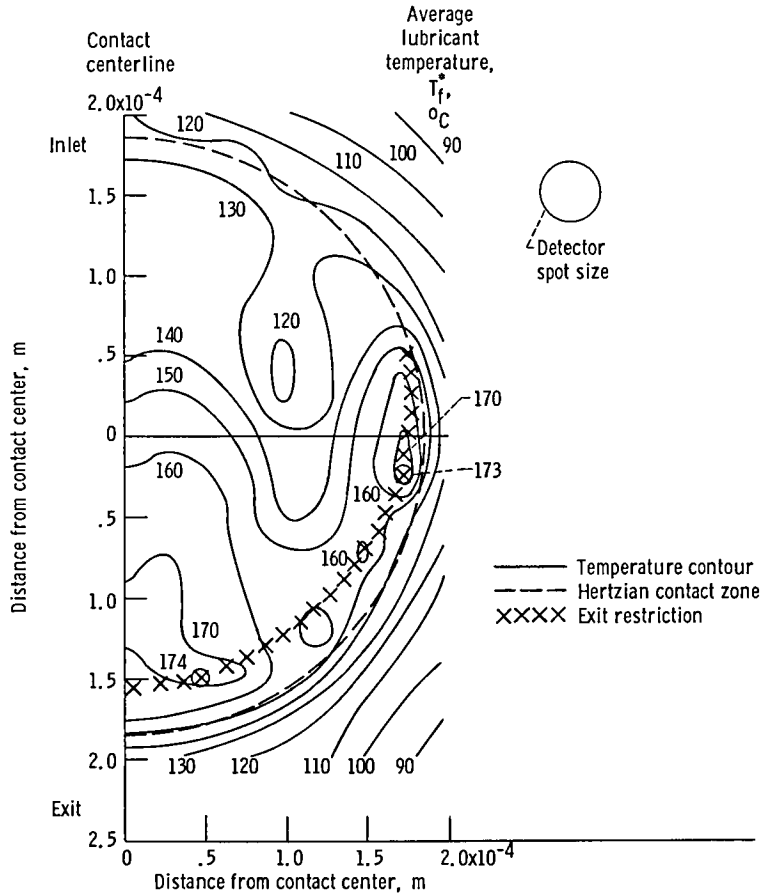

Figure 10.19. - Average lubricant temperature. Sliding speed, u, 1.4 m/s; load, F, 67 N; maximum Hertzian pressure, P_{Hz}, 1.0 GN/m^2. (From Ausherman, et al., 1976.)

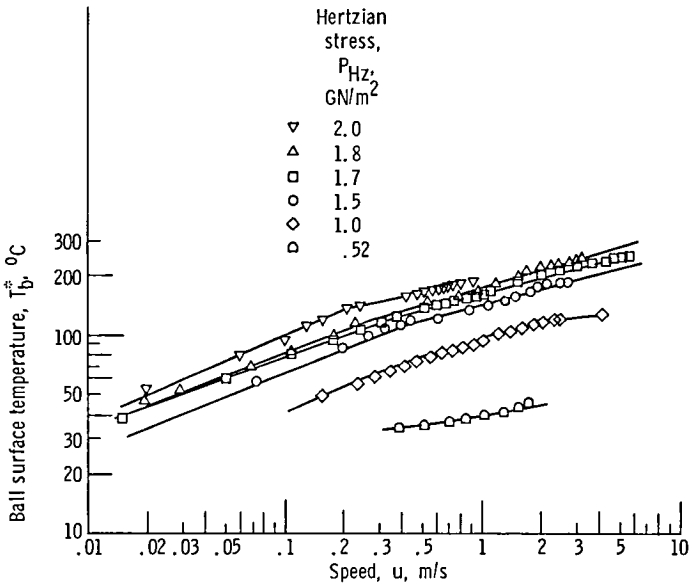

Figure 10.20. - Effect of speed on ball surface temperature. Ratio of film thickness to composite surface roughness, Λ, >2 except at 2.0-GN/m^2 load, where $1 < \Lambda < 2$. (From Ausherman, et al., 1976.)

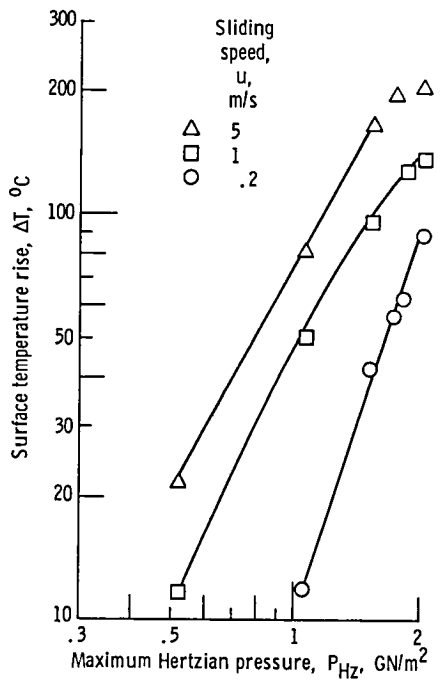

Figure 10.21. - Effect of maximum Hertzian pressure on surface temperature rise. (From Ausherman, et al., 1976.)

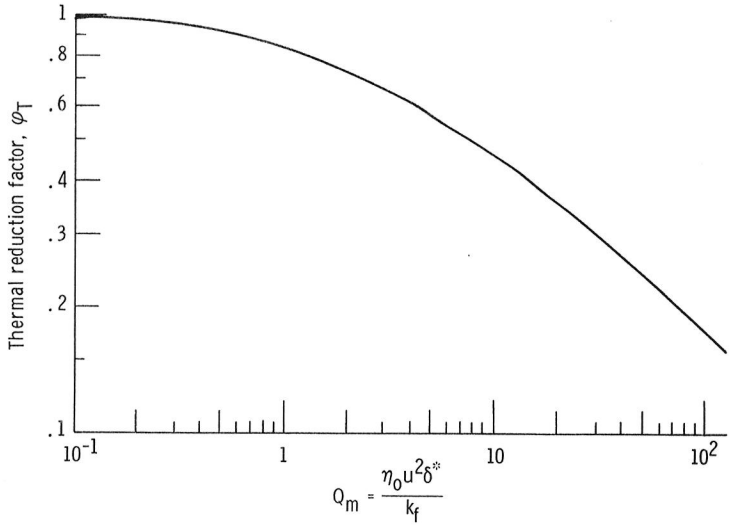

Figure 10.22. - Thermal reduction factor. (From Cheng, 1967.)

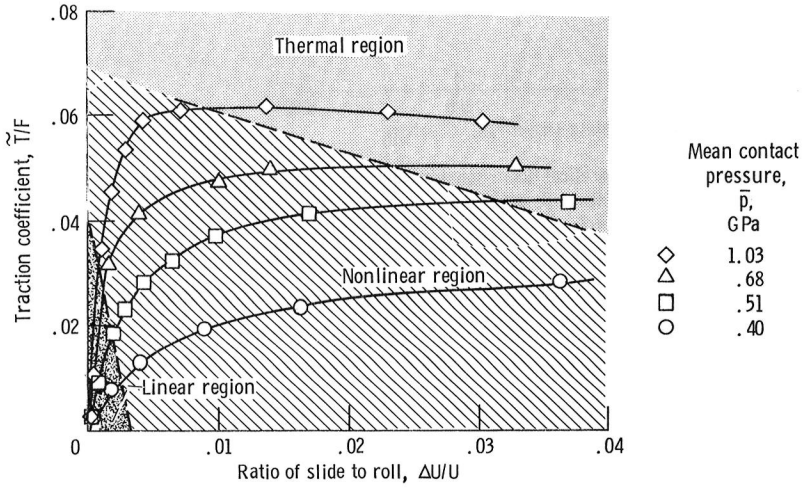

Figure 10.23. - Typical curves of traction measured on two-disc machine in line contact. (From Johnson and Cameron, 1967.)

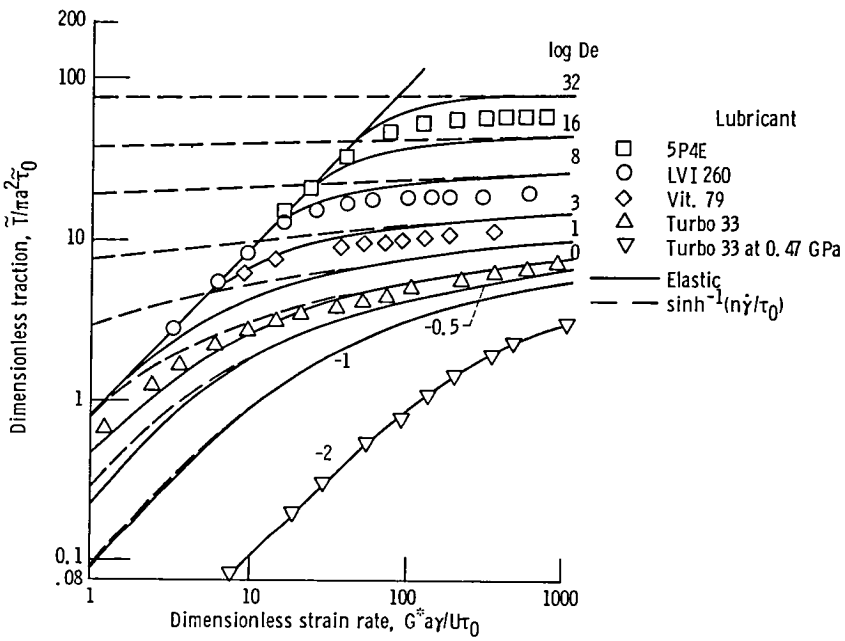

Figure 10.24. - Theoretical nondimensional traction curves for varying Deborah number. Mean contact pressure, $\bar{p}$, 0.67 GPa; spin-roll ratio, e, 30^0 to 40^0. (From Johnson and Tevaarwerk, 1977.)

1. Report No.	2. Government Accession No.	3. Recipient's Catalog No.
NASA TM-81698		

4. Title and Subtitle	5. Report Date
Experimental Investigations of Elastohydrodynamic Lubrication	May 1983
	6. Performing Organization Code: 505-32-42
7. Author(s): Bernard J. Hamrock and Duncan Dowson	8. Performing Organization Report No.: E-209
	10. Work Unit No.
9. Performing Organization Name and Address: National Aeronautics and Space Administration, Lewis Research Center, Cleveland, Ohio 44135	11. Contract or Grant No.
	13. Type of Report and Period Covered: Technical Memorandum
12. Sponsoring Agency Name and Address: National Aeronautics and Space Administration, Washington, D.C. 20546	14. Sponsoring Agency Code

15. Supplementary Notes

Bernard J. Hamrock, NASA Lewis Research Center, Cleveland, Ohio; Duncan Dowson, Institute of Tribology, Department of Mechanical Engineering, The University of Leeds, Leeds, England. Published as Chapter 10 in Ball Bearing Lubrication by Bernard J. Hamrock and Duncan Dowson, John Wiley & Sons, Inc., September 1981.

16. Abstract

Various experimental studies of elastohydrodynamic lubrication have been reviewed. The various types of machines used in these investigations - such as the disc, two- and four-ball, crossed-cylinders, and crossed-axes rolling disc machines - have been described. The measurement of the most important parameters - such as film shape, film thickness, pressure, temperature, and traction - has been considered. Determination of the film thickness is generally the most important of these effects since it dictates the extent to which the asperities on opposing surfaces can come into contact and thus has a direct bearing on wear and fatigue failure of the contacting surfaces. Several different techniques for measuring film thickness have been described - including electrical resistance, capacitance, X-ray, optical interferometry, laser beam diffraction, strain gage, and spring dynamometer methods. An attempt has been made to describe the basic concepts and limitations of each of these techniques. These various methods have been used by individual researchers, but there is no universally acceptable technique for measuring elastohydrodynamic film thickness. Capacitance methods have provided most of the reliable data for nominal line or rectangular conjunctions, but optical interferometry has proved to be the most effective procedure for elliptical contacts. Optical interferometry has the great advantage that it reveals not only the film thickness, but also details of the film shape over the complete area of the conjunction. Theoretical film thickness solutions developed elsewhere and the various experimental techniques available for measuring this important parameter have been described. This has been followed by a comparison of theoretical and experimental findings from various sources, and a pleasing agreement between the two has been noted. Attention has also been focused on experimental studies of other important aspects of elastohydrodynamic lubrication - such as pressure distribution, the temperature rise on the surface of the solids and within the lubricant, and traction.

17. Key Words (Suggested by Author(s))	18. Distribution Statement
Experimental machines Elastohydrodynamic lubrication Traction measurements Temperature measurements	Unclassified - unlimited STAR Category 37

19. Security Classif. (of this report)	20. Security Classif. (of this page)	21. No. of pages	22. Price*
Unclassified	Unclassified		

*For sale by the National Information Service, Springfield, Virginia 22161

National Aeronautics and
Space Administration

Washington, D.C.
20546

Official Business
Penalty for Private Use, $300

SPECIAL FOURTH CLASS MAIL
BOOK

Postage and Fees Paid
National Aeronautics and
Space Administration
NASA-451

NASA

POSTMASTER: If Undeliverable (Section 158
Postal Manual) Do Not Return